Chemical Science

ROYAL SOCIETY OF CHEMISTRY

REVIEW

View Article Online
View Journal | View Issue

Cite this: *Chem. Sci.*, 2025, **16**, 11740

Pore engineering in metal–organic frameworks and covalent organic frameworks: strategies and applications

Yanpei Song and Shengqian Ma *

Crystalline porous materials, particularly metal–organic frameworks (MOFs) and covalent organic frameworks (COFs), have garnered significant attention for advanced applications due to their tunable pore environments and versatile functionalities. By precisely controlling factors such as size, shape, functional sites, and pore distribution, MOFs and COFs can be tailored to exhibit high selectivity for specific molecules, making them ideal for applications in gas storage and separation, catalysis, and water remediation. This review provides a background overview, beginning with an introduction to pore surface engineering strategies and the design features of MOFs and COFs. It then highlights recent advancements in three key research areas that our group has investigated in-depth over the past decade, discussing the strategies and principles involved. Finally, we outline the remaining challenges and offer our perspectives on future opportunities for pore-engineered MOFs and COFs.

Received 28th February 2025
Accepted 11th June 2025

DOI: 10.1039/d5sc01635e

rsc.li/chemical-science

1. Introduction

The intriguing properties of crystalline porous materials, including zeolites,[1–3] metal–organic frameworks (MOFs),[4–9] covalent organic frameworks (COFs),[10–15] and hydrogen-bonded organic frameworks (HOFs),[16–20] have drawn significant interest from diverse research fields over the past several decades. Among these crystalline porous materials, MOFs and COFs have attracted particular attention due to their highly tunable structures.[21–23] Unlike traditional porous materials such as activated carbon,[24] molecular sieves,[25] and mesoporous silica,[26] which often exhibit limited structural regularity, poorly defined pore architectures, and minimal chemical tunability, MOFs and COFs offer precise control over pore size, shape, connectivity, and surface functionality. Their modular construction, based

Department of Chemistry, University of North Texas, Denton, TX 76201, USA. E-mail: Shengqian.Ma@unt.edu

Yanpei Song

Yanpei Song received his BS from Beijing University of Chemical Technology, China in 2017, and graduated from the University of North Texas with a PhD degree in 2023 under the supervision of Prof. Shengqian Ma. Since 2023, he has been a postdoctoral research associate in the Nanomaterials Chemistry Group, Chemical Science Division at Oak Ridge National Laboratory. His research interests focus on the development of functional covalent organic frameworks, and porous organic polymers for environmental remediation and precious metal recovery.

Shengqian Ma

Shengqian Ma obtained his BS degree from Jilin University in 2003 and graduated from Miami University with a PhD Degree in 2008. After finishing a two-year Director's Postdoctoral Fellowship at Argonne National Laboratory, he joined the Department of Chemistry at University of South Florida as an Assistant Professor in 2010 and was promoted to Associate Professor with early tenure in 2015 and to Full Professor in 2018. In August 2020, he joined the University of North Texas as the Robert A. Welch Chair in Chemistry. His current research interest focuses on the task-specific design and functionalization of advanced porous materials for energy-, biological-, and environmental-related applications.

on the selection of organic linkers and metal or covalent nodes, enables the formation of frameworks with diverse and well-defined pore structures. This high degree of structural programmability has driven a surge in the development of novel porous materials with broad applicability across various fields.

MOFs are a class of hybrid organic–inorganic crystalline materials composed of metal ions or metal clusters (nodes) connected by organic ligands (linkers) through coordination bonds. The vast combinational possibilities between metals and organic ligands result in a wide range of structures with highly tunable properties. In contrast, COFs are fully organic crystalline porous materials composed of organic building blocks connected *via* strong covalent bonds (*e.g.*, C=N, C=C, B–O bonds). Unlike MOFs, which have metal nodes, COFs are constructed entirely from organic molecules, resulting in lightweight structures with higher thermal and chemical stability. Recently, a new class of crystalline porous materials, covalent metal–organic frameworks (CMOFs), has emerged, combining the key features of both MOFs and COFs. CMOFs integrate the structural precision and covalent connectivity of COFs with the functional versatility and catalytic potential of metal centers in MOFs.[27]

The distinctive morphologies and tunable pore surface chemistries of MOFs and COFs not only provide exceptionally large internal surface areas—up to approximately 7839 $m^2\ g^{-1}$ for MOFs[28] and 5083 $m^2\ g^{-1}$ for COFs[29]—with uniform pore channels and windows, but also endow them with versatile pore functionalities, making them highly suitable for various industrial applications such as gas storage and separation,[30–37] heterogeneous catalysis,[38–44] proton conduction,[45–49] chemical sensing,[50–56] and environmental remediation.[57–62] Abundant opportunities for tailoring their pore surfaces through pore engineering can be readily achieved through a wide range of chemical strategies, from *de novo* design of organic linkers and connecting nodes to post-synthetic modifications (PSMs).[63–69] *De novo* synthesis allows precise control over pore size, shape, and connectivity by designing functionalized linkers/monomers and metal nodes, while PSM enables the introduction of specific functional moieties or active sites into pre-formed frameworks. Additionally, sophisticated engineering techniques, such as pore space partitioning and hierarchical pore construction, can further optimize their performance. Pore surface modification, such as grafting functional groups or catalytic sites, enables the alignment of ordered active centers within the pores, facilitating selective molecular interactions. Meanwhile, partitioning or sub-framework assembly can tune the pore environment to accommodate target analytes based on their molecular size, polarity, or electronic properties. These tailored modifications are particularly crucial for meeting industrial requirements, such as selectively storing or separating desired products from complex mixtures, especially small-molecule gases (*e.g.*, H_2, CO_2, CH_4). The synergy between rational framework design and advanced post-synthetic engineering highlights the tremendous potential of MOFs and COFs in addressing critical challenges in energy, environment, and chemical industries.

2. Pore surface engineering

Pore engineering refers to a comprehensive set of processes aimed at modifying the pore structures of MOFs and COFs. These processes include the construction, combination, functionalization, and partitioning of pores at the unit cell level. Additionally, pore engineering can involve the generation of hierarchical pore structures—ranging from micro to meso and even macro pores—within the framework. The primary goal of pore engineering is to optimize the pore characteristics of MOFs and COFs, ensuring that these materials meet the specific requirements of various applications. This optimization typically involves introducing specific functional sites or guest species into targeted pore positions. These species are often immobilized through covalent bonds or coordination interactions, which help tune the chemical environment or morphology of the pore surface. By carefully controlling the pore structure and its chemistry, pore engineering enables the precise customization of the material's properties, making it adaptable to a broad range of applications.

Through the pore engineering methodology, MOFs and COFs can be endowed with a variety of versatile pore features, including enhanced surface areas, controlled pore sizes, and specialized functionalities. This level of customization enables the materials to be tailored for specific industrial applications. Additionally, pore engineering acts as a powerful tool for developing crystalline porous materials with targeted, application-specific properties, driving innovation across a wide range of scientific and industrial fields.

2.1 *De novo* design of linkers and connecting nodes

The fundamental principle of pore construction in MOFs lies in the careful selection of metal clusters and organic ligands, following a bottom-up synthetic approach. The formation of these metal clusters is highly dependent on experimental conditions, including the choice of metal precursors, solvent during the solvothermal process, and reaction temperature. The pioneering MOF structures reported by Yaghi's group, MOF-2 and MOF-5, showcase how differences in coordination modes under varying synthetic conditions can lead to distinct pore architectures.[70,71] Both MOFs are constructed from zinc(II) clusters and 1,4-benzenedicarboxylic acid (H_2BDC) as the organic ligand. However, MOF-2 features $Zn_2(COO)_4$ paddle-wheel units, while MOF-5 forms $Zn_4O(COO)_6$ secondary building units (SBUs). This difference in coordination geometry results in contrasting pore topologies: MOF-2 adopts a 2D layered structure with lower surface area and less accessible porosity, whereas MOF-5 forms a 3D open framework, offering a higher surface area and greater porosity. These structural distinctions highlight how synthetic control over metal–ligand coordination plays a crucial role in tuning the porous properties and functional potential of MOFs.

Incorporating mixed metals is a common strategy to adjust framework flexibility, tune pore chemistry and functionality, and introduce additional active sites. The simplest method for synthesizing mixed-metal MOFs (MM-MOFs) is a direct one-pot

solvothermal synthesis using a mixture of different metal precursors. However, this approach often lacks precise control over metal distribution, leading to challenges such as uneven metal arrangement, where one metal species may dominate the connecting nodes, while the other forms (hydroxy)oxide clusters on the pore surfaces instead of integrating into the framework. To address this challenge, selecting metals with similar coulombic charges, ionic radii, and chemical behaviors are essential for achieving a uniform metal distribution within the framework.[72] Wang *et al.* successfully incorporated up to 10 different divalent metals (Mg, Ca, Sr, Ba, Mn, Fe, Co, Ni, Zn, and Cd) into microcrystalline MOF-74 *via* a one-pot solvothermal reaction, demonstrating the feasibility of controlled metal integration (Fig. 1).[73] By optimizing metal–ligand coordination, reaction conditions, and precursor compatibility, the development of mixed-metal MOFs (MM-MOFs) with enhanced pore functionality, diverse active sites, and improved performance in applications such as gas storage, separation, and catalysis becomes achievable.

The use of multiple linkers (mixed linkers) to modify the functionality and pore structure of MOFs is a highly effective strategy for achieving precise pore engineering. This approach is relatively easy to implement because different ligands often share the same coordination mode with metal nodes, differing only slightly in their functional groups. The pioneering work on multivariate (MTV) MOFs was reported by Deng *et al.*, who successfully synthesized MTV-MOF-5 using up to eight different linkers in a one-pot reaction, resulting in a single-phase MTV-MOF-5 crystal.[74] In their approach, all selected ligands had identical lengths and coordination sites, ensuring their orderly incorporation into a single MOF crystal without disrupting the framework structure. This multivariate linker strategy was subsequently extended to the development of MTV-COFs, where up to four different monomers with various functionalities were uniformly incorporated into a single-phase COF crystal (Fig. 2).[75] The successful distribution of multiple building blocks in both MTV-MOFs and MTV-COFs highlights the versatility of this approach for customizing pore environments and tuning material properties for diverse applications.[76,77]

In contrast to MOFs, which have connecting nodes formed through coordination bonds, COFs are typically constructed from reversible covalent bonds *via* dynamic covalent reactions (DCRs). During COF formation, processes such as bond formation, bond cleavage, and bond exchange occur simultaneously under appropriate conditions. This ongoing dynamic bond breaking and reformation allows the framework to undergo self-healing, effectively repairing defects and resulting in highly ordered pore structures and highly crystalline frameworks. The pore chemistry of COFs can be readily tuned by introducing different linkage units, even when maintaining the same rigid skeleton, enabling the design of COFs with diverse functionalities. The first successful synthesis of COFs *via* reversible reactions was achieved by Yaghi in 2005, who utilized boronic ester condensation (*e.g.*, boronic ester and boroxine formation).[78] This breakthrough not only demonstrated the self-healing ability of purely organic frameworks but also yielded the first porous, crystalline, covalent organic frameworks (COFs). Following this pioneering work, other reversible reactions, particularly Schiff-base condensations (*e.g.*, imine, hydrazone, azine, and Salen linkages),[79–86] have become prominent in COF synthesis. Among these, imine-linked COFs have gained notable success due to their high thermal and chemical stability, as well as their broad chemical tunability, derived from the vast selection of functional amines and aldehydes, making them highly suitable for various task-specific applications. Moreover, imine-linked COFs can undergo PSMs to yield specifically evolved functional COFs, further enhancing their properties and expanding their application potential across diverse research fields.

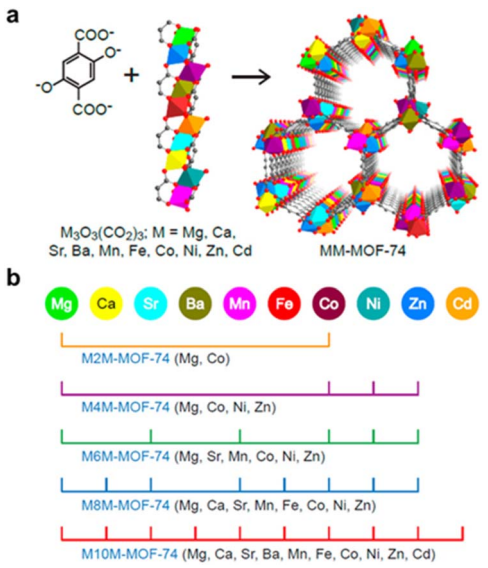

Fig. 1 (a) Schematic illustration of synthesizing MM-MOF-74. (b) Combination of metal ions used to synthesize MM-MOF-74. Reproduced with permission.[73] Copyright 2014, American Chemical Society.

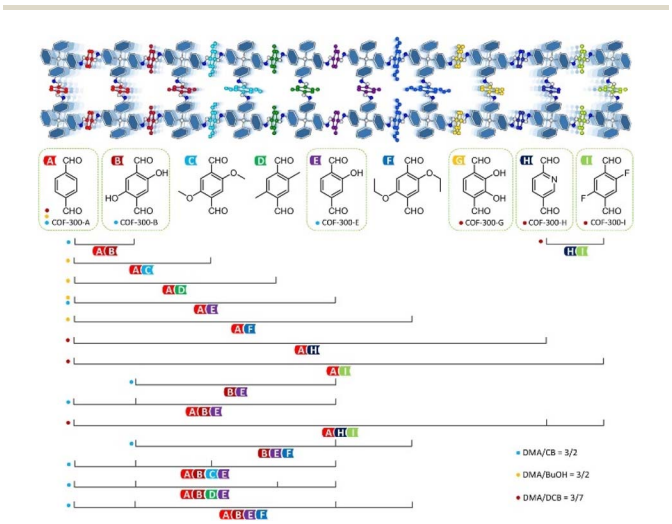

Fig. 2 Construction of single-linker COFs and MTV-COFs through pure linkers or mixed linkers and the influence of solvent combinations on their synthesis. Reproduced with permission.[75] Copyright 2023, American Chemical Society.

In recent years, irreversible covalent bonds have been increasingly employed to construct COFs with enhanced stability, enabling their application under harsh conditions. Several types of irreversible linkages, including β-ketoenamine,[87–89] polyimide,[90–92] imidazole,[93–95] and benzoxazole,[96–98] are primarily derived from imine-based chemistry.[99] Among these, β-ketoenamine-linked COFs have emerged as one of the most popular platforms for pore engineering, thanks to their high crystallinity and synthetic feasibility. Beyond imine-derived linkages, vinylenes and fused heterocycle linkages are two additional types of irreversible bonds widely employed for constructing ultrastable COFs.[100–104] The Feng group[105] and Jiang group[106] reported pioneering examples of vinylene-linked COFs in 2016 and 2017, respectively, using the Knoevenagel condensation reaction to form carbon–carbon double bonds. Subsequently, the aldol condensation reaction[107] and the Horner–Wadsworth–Emmons reaction,[108] both involving aldehyde monomers and active methyl groups, were developed to expand the library of vinylene-linked COFs, further enhancing their synthetic versatility. In another notable advancement, Thomas *et al.* introduced the concept of covalent triazine frameworks (CTFs),[109] synthesizing a series of triazine-linked polymers *via* highly dynamic condensation reactions. The C=N aromatic linkages (triazine units) in CTFs, fused through –CN units, impart these frameworks with high chemical stability, rich nitrogen content, and expanded practical applications, particularly in heterogeneous catalysis and gas storage.[110–112] Additionally, other fused heterocycle linkages, such as dioxin,[113–115] piperazine,[116,117] pyrazine,[118] and thiazole,[119,120] have been employed to construct ultrastable COFs with excellent acid- and base-resistance. Moreover, these fused-ring structures generally exhibit enhanced electrical conductivity compared to imine-linked COFs, making them highly promising candidates for electrocatalysis and other electrochemical applications. Collectively, the development of irreversible linkages in COFs has significantly broadened their structural diversity, chemical robustness, and functional tunability, driving their deployment in demanding industrial and scientific applications.

Recently, CMOFs have emerged as a promising class of crystalline porous materials that integrate the advantages of MOFs and COFs. Their synthesis typically involves assembling metal complexes or clusters with functional groups (*e.g.*, –CHO, $–NH_2$), which then react with organic linkers *via* dynamic covalent chemistry to form extended networks. This approach combines the functional versatility of metal centers with the high chemical stability of covalent bonds. The *de novo* design of linkers and connecting nodes is central to CMOF development. By tailoring the geometry and reactivity of organic linkers and metal-based precursors, it is possible to control the framework structure, pore environment, and overall functionality. Li's group has established a versatile strategy for constructing CMOFs by synthesizing cyclic trinuclear units (CTUs) based on coinage metals (Cu, Ag, Au), which are functionalized with reactive groups.[121–128] These CTUs can undergo covalent linkage with a variety of organic monomers, leading to CMOFs with tunable structures and properties, such as redox activity, luminescence, metallophilic interactions, and catalytic functionality. As such, CMOFs offer a robust platform for developing stable and multifunctional porous materials with promising applications in catalysis, sensing, and energy conversion.

2.2 Post-synthetic modifications for tailoring pore chemistry

PSMs offer a powerful and versatile approach to tailoring the pore chemistry of MOFs and COFs, expanding their functionality beyond what is achievable through direct synthesis.[129–132] Unlike *de novo* synthesis, which requires precise control over precursor design and reaction conditions, PSMs enable the site-selective incorporation of functional groups that are otherwise difficult to introduce during initial framework formation. This allows for fine-tuning of host–guest interactions, enhancing selectivity and efficiency in applications such as gas storage, molecular separation, catalysis, proton conduction, and sensing. Beyond functionalization, PSMs play a crucial role in reinforcing structural stability, making MOFs and COFs more resistant to moisture, acids, bases, and high temperatures. By modifying reactive sites or strengthening framework linkages, PSMs prevent framework degradation and improve material robustness under harsh operational conditions. This is particularly beneficial for COFs, where dynamic imine bonds can be post-synthetically converted into stronger covalent linkages such as amide and fused heterocyclic bonds, significantly enhancing chemical and thermal stability.[133] Moreover, PSMs facilitate hierarchical pore engineering, allowing precise control over pore size, shape, and surface chemistry to accommodate specific molecular targets. This has profound implications for gas separation, biomolecular recognition, drug delivery, and size-selective catalysis, where optimized pore environments are essential for performance. By leveraging a diverse range of PSM techniques, including oxidation, hydrolysis, acylation, and cross-linking reactions, researchers can systematically enhance both the functionality and durability of MOFs and COFs, broadening their practical applications across multiple scientific and industrial fields.

Despite these advantages, PSMs also present several limitations that need to be addressed to fully realize their potential: (1) incomplete or non-uniform functionalization often occurs due to steric hindrance or limited diffusion of modifiers within the framework, leading to heterogeneous surface chemistry and inconsistent performance; (2) excessive or bulky grafting can cause pore blockage and reduced accessible surface area, thereby compromising adsorption and transport properties; (3) certain post-modification reactions—especially those involving harsh reagents or conditions—may induce partial framework degradation, particularly in less robust MOFs; (4) the precise characterization of modification degree and location within confined pore environments remains challenging, hindering the rational design of structure–property relationships. To overcome these issues, several strategies can be adopted: the use of small, highly reactive modifiers and optimized solvent systems can improve the uniformity of functionalization; controlling grafting density and selecting appropriately sized modifiers help preserve porosity; employing mild reaction

conditions and orthogonal chemistries can maintain structural integrity; and advanced characterization tools such as solid-state nuclear magnetic resonance, synchrotron-based X-ray techniques, and vibrational spectroscopy can offer deeper insight into the spatial distribution and extent of functionalization.

2.2.1 Post-synthetic exchange of metal, ligand, or monomer. The post-synthetic exchange (PSE) method provides a viable strategy for metal ion exchange in pre-formed MOF frameworks, leading to the formation of mixed-metal MOFs (MM-MOFs) that are often difficult to achieve through direct synthesis.[134,135] This approach allows for the controlled incorporation of secondary metal ions into pre-formed frameworks while maintaining their structural integrity and crystallinity. However, successful cases of metal exchange in MOFs are still relatively limited, as the process is often strongly influenced by factors such as the rigidity of the framework, the strength of the metal–ligand bonds, and the compatibility of the solvent system. A pioneering example was reported by Das *et al.*, who demonstrated the first complete and reversible exchange of metal ions within a robust microporous MOF while maintaining its single crystallinity.[136] This study provided direct evidence that metal ion exchange in rigid frameworks is feasible and can be precisely controlled. Building upon this, Song *et al.* successfully synthesized an MM-MOF *via* metal ion exchange in Zn-HKUST-1, where up to 56% of the Zn(II) ions in the framework were replaced by Cu(II) ions in a methanol solution.[137] However, this process was found to be irreversible, as soaking the transmetalated $Cu_{0.56}Zn_{0.44}$-HKUST-1 in a Zn(II)-methanol solution did not lead to the reincorporation of Zn(II) ions back into the framework. Further advancing this strategy, Dincă's group applied a similar soaking method to partially replace Zn(II) ions in MOF-5.[138] By exchanging the $Zn_4O(COO)_6$ clusters, they successfully introduced a range of transition metals, creating $MZn_3O(COO)_6$ clusters with M = V^{2+}, Ti^{3+}, Cr^{2+}, Cr^{3+}, Mn^{2+}, and Fe^{2+}. This study highlighted the versatility of PSE in diversifying MOF composition, allowing for tunable electronic, catalytic, and adsorption properties. Although PSE has proven effective for metal exchange, challenges such as selectivity, reversibility, and control over metal distribution remain significant obstacles. Future developments in solvent engineering, ligand design, and reaction kinetics could further expand its applicability, offering new avenues for designing functionalized MM-MOFs with target applications.

Ligand exchange, a key PSM strategy, has emerged as a powerful method for incorporating multiple functionalities into MOFs, leading to the formation of MTV-MOFs. Unlike *de novo* synthesis, which requires precise control over precursor compatibility, ligand exchange allows for the substitution of organic linkers in a pre-formed MOF without disrupting its overall framework integrity. This method provides a versatile route for introducing functional diversity, modifying pore environments, and tuning MOF properties for specific applications. In ligand exchange, pre-assembled MOFs are immersed in a solution containing new ligands, which gradually replace the original linkers through thermodynamic and kinetic exchange processes. The feasibility of this method depends on several factors, including the stability of the framework, the binding affinity of the incoming ligands, and solvent compatibility. Li *et al.* demonstrated a stepwise ligand exchange strategy to prepare a series of isoreticular bio-MOF-100 analogues (Fig. 3).[139] In this approach, the ligand 2,6-naphthalenedicarboxylate (NDC), originally used to construct bio-MOF-101, was replaced by 4,4′-biphenyldicarboxylate (H_2BPDC) through a controlled soaking process. Specifically, bio-MOF-101 was immersed in an H_2BPDC/DMF/NMP solution at 75 °C for a set duration, leading to its transformation into bio-MOF-100. This method was further employed to expand the pores of bio-MOF-100 by substituting BPDC with longer organic linkers, including azobenzene-4,4′-dicarboxylate (ABDC) and 2′-amino-1,1′:4, 1″-terphenyl-4,4″-dicarboxylate (NH_2-TPDC), thereby fine-tuning the pore size and functionality. The same post-synthetic ligand exchange strategy, involving the immersion of solid MOFs in a solution containing a secondary ligand, has also been successfully applied to zeolitic imidazolate frameworks (ZIFs). Cohen's group reported that in ZIF-71(Zn), the 4,5-dichloro-imidazole ligand could be partially replaced by 4-bromo-1*H*-imidazole *via* solid–liquid PSE.[140] Furthermore, Cohen's group extended the ligand exchange approach to solid-state reactions, demonstrating that post-synthetic ligand exchange could occur between two distinct MOFs under relatively mild conditions. This was exemplified with UiO-66(Zr),[141] MIL-53(Al), and MIL-68(In),[142] where ligand exchange was successfully achieved through solid–solid PSE. For instance, in the case of MIL-53(Al), two functionalized derivatives, one synthesized using BDC-NH_2 (aminated) and the other using BDC-Br (brominated), were physically mixed in water and

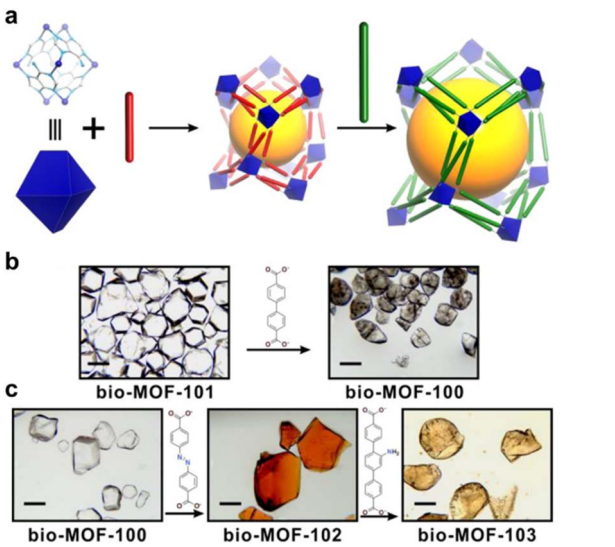

Fig. 3 Scheme illustrating the pore expansion strategy. (a) As-synthesized bio-MOF-101 was converted to bio-MOF-100 through ligand exchange with BPDC. (b) BPDC in bio-MOF-100 was subsequently replaced with ABDC to form bio-MOF-102, followed by the replacement of ABDC in bio-MOF-102 with NH2-TPDC to yield bio-MOF-103. (c) Light microscope images of the crystalline MOFs, with scale bars representing 0.2 mm. Reproduced with permission.[139] Copyright 2013, American Chemical Society.

incubated at 85 °C (a significantly lower temperature than the original solvothermal synthesis at 150 °C) for five days. Aerosol time-of-flight mass spectrometry (ATOFMS) analysis confirmed that the chemical composition of the framework had been altered, providing strong evidence that solid–solid PSE had successfully occurred within the MIL-53(Al) derivatives. These studies highlight the versatility and effectiveness of ligand exchange as a PSM technique, allowing for precise control over MOF pore environments, functionality, and framework composition, while maintaining structural integrity.

Similar to ligand exchange in MOFs, monomer exchange in COFs has been explored as a strategy to construct COFs with more complex structures. Qian *et al.* developed an *in situ* COF-to-COF transformation approach, where the benzidine linkers in TP-COF-BZ were selectively replaced with 1,4-diaminobenzene linkers under solvothermal conditions (Fig. 4a).[143] This method enabled the controlled generation of COFs with three distinct types of pores, demonstrating the potential of monomer exchange for tailoring COF architectures at the solid-state level. Wang and coworkers further advanced this concept by introducing a self-limited dynamic linker exchange strategy for surface functionalization of uniform COF microspheres (Fig. 4b).[144] Their approach allowed for precise modification of COF surfaces while preserving the overall morphology. Specifically, they selected six different monomers with varying functional groups and linker lengths, enabling the transformation of a parent COF microsphere (PCOF) into six distinct functionalized COF microspheres, which was originally synthesized *via* the Schiff-base condensation of 1,3,5-tris(4-aminophenyl)benzene (TPB) and 2,5-dimethoxyterephthalaldehyde (DMTP). This strategy significantly enriched the library of COF microspheres, offering a versatile approach to tune COF properties for diverse applications.

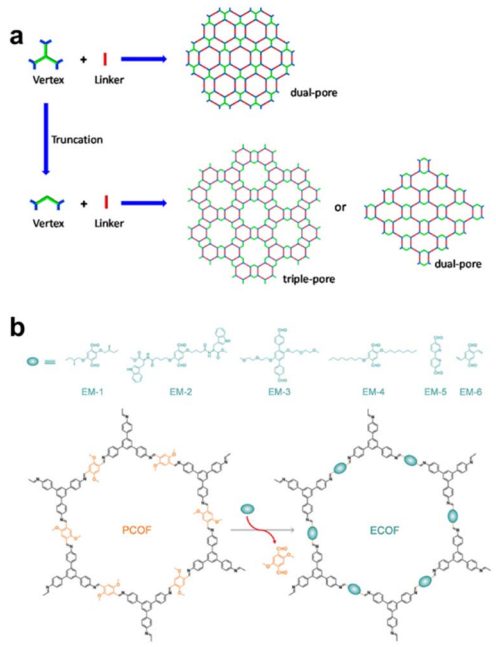

Fig. 4 (a) Precise construction of dual-pore COFs *via* a multiple-linking-site strategy and fabrication of triple-pore COFs through the integration of vertex-truncation design with the multiple-linking-site strategy. Reproduced with permission.[143] Copyright 2017, American Chemical Society. (b) Structures of six functional linkers and a schematic illustration of the *in situ* linker exchange process for functionalizing ECOF stationary phases. Reproduced with permission.[144] Copyright 2024, John Wiley and Sons.

2.2.2 Functional group grafting for pore environment modulation. Another widely used PSM strategy for grafting functional groups or active sites onto the pore surfaces of MOFs and COFs involves immobilizing functional species through coordinated or covalent bonds. This approach is highly effective for precisely tuning the pore chemistry without compromising the structural integrity of the framework, thereby significantly expanding the versatility and applicability of these materials across various fields. In MOFs, the pore chemistry modification can be achieved by coordinating metal complexes, organocatalysts, or solvent molecules to open metal sites (OMSs) or by covalently modifying organic linkers to introduce hydrophilic, hydrophobic, or reactive moieties for enhanced guest interactions. In COFs, covalent post-modifications such as imine-to-amide conversion, click chemistry, and acylation enable robust functionalization, enhancing chemical stability and selectivity for various applications. These tailored modifications not only optimize host–guest interactions but also improve framework durability, making PSM an indispensable tool for developing task-specific porous materials with tunable properties.

A number of MOF structures possess the ability to release auxiliary ligands from their metal ion nodes, often leading to the formation of coordinatively unsaturated metal centers. These OMSs can subsequently coordinate with other molecules, thereby introducing new functionalities or modulating pore geometries. One of the earliest demonstrations of this phenomenon was reported in 1999 by Williams and co-workers, who investigated the well-known HKUST-1 compound.[145] Their study revealed that a partial building block ligand, 1,3,5-benzenetricarboxylate (BTC), on the paddle-wheel SBUs of HKUST-1, could be replaced by pyridine upon treatment with dry pyridine. This replacement occurred due to the lability of the axial aqua ligands, yet the 3D lattice of the MOF remained intact. This PSM not only altered the pore structure and chemistry of HKUST-1 but also introduced tunable functionalization at the metal nodes. Interestingly, the study demonstrated that pyridine-decorated HKUST-1 could not be obtained through direct solvothermal synthesis from Cu(II) salts, BTC, and pyridine, but could be successfully prepared *via* post-synthetic modification, thereby highlighting the unique advantage of MOFs as structurally robust and tunable platforms. This ability to precisely tailor the local microenvironment through ligand exchange greatly enhances the versatility and functional adaptability of these materials.

Both the ligands in MOFs and the monomers in COFs can be readily functionalized with additional groups through coordinated or covalent interactions, significantly expanding their structural diversity and functional tunability. Among these, 2,2′-bipyridyl (bpy) is a widely used chelating ligand for transition metal (TM) complexes due to its strong coordination ability and

electronic properties. Carboxylate-functionalized bpy derivatives have been extensively explored as either pre-integrated or post-modified ligands for MOF synthesis with various metal salts, enabling the precise incorporation of catalytically active metal centers. Yaghi's group pioneered the incorporation of metal sites into MOF-253, a framework featuring open 2,2′-bpy coordination sites.[146] MOF-253 was synthesized from 2,2′-bipyridine-5,5′-dicarboxylic acid (bpydc) and $AlCl_3$ in DMF, followed by post-synthetic metalation with $PdCl_2$ and $Cu(BF_4)_2$ in MeCN solution to yield bimetallic MOFs. This strategy allowed for the controlled introduction of catalytically active metal centers, significantly enhancing the material's functional versatility. Building on this concept, Lin's group reported the synthesis of chemically stable and recyclable bpy-UiO-Pd and bpy-UiO-Ir by treating a UiO-type MOF containing bipyridyl moieties (bpy-UiO) with Pd and Ir precursors.[147] Notably, bpy-UiO-Ir exhibited exceptional catalytic activity in the dehydrogenative borylation of aromatic C–H bonds using $B_2(pin)_2$ (pin = pinacolate) as the borylating agent, highlighting the potential of MOFs containing nitrogen donor ligands as highly stable and efficient catalysts for key organic transformations. These studies underscore the effectiveness of post-synthetic metalation in tailoring MOFs for specific catalytic applications.

Beyond MOFs, the bpy moiety has also been widely employed in COF frameworks to immobilize metal sites, enabling the design of highly recyclable and structurally robust catalysts. Our group developed an effective strategy for incorporating metal-active sites into COFs by synthesizing COF-TpBpy through the condensation of 1,3,5-triformylphloroglucinol (Tp) and 5,5′-diamino-2,2′-bipyridine (Bpy), followed by coordination with Cu sites (Fig. 5).[148] Additionally, flexible polymeric phosphonium salts (PPS) were confined within the COF channels *via in situ* polymerization. The resulting material, PPS ⊂ COF-TpBpy-Cu, leveraged the mobility of catalytically active sites on the highly flexible PPS, along with synergistic interactions between the polymeric moieties and Lewis acid sites (Cu species) anchored on the COF walls. This unique system exhibited superior catalytic performance in the cycloaddition of epoxides with CO_2 to form cyclic carbonates, demonstrating enhanced reactivity and recyclability. This work not only unveils a novel strategy for designing bifunctional catalysts with dual activation behavior but also opens new avenues for developing multifunctional systems that mimic biocatalysis. To date, numerous functionalized bipyridine-based COFs have been reported, incorporating a range of metal sites including Co, Ni, Cu, Pd, Ru, Rh, Re, and Ir, among others.[149,150] These metallized bpy-based COFs have exhibited significant potential for various catalytic applications, such as asymmetric catalysis, electrocatalysis, photocatalysis, and small-molecule activation. The tunability of the bpy-metal coordination environment, coupled with the high stability and porosity of COFs, continues to drive innovations in designing next-generation porous catalysts for sustainable chemical transformations.

The Salen unit is one of the most significant ligands in coordination chemistry, widely utilized for the design of metal–organic frameworks (MOFs) and covalent organic frameworks (COFs) due to its strong coordination ability and structural versatility.[151] Wang and coworkers were the first to report the construction of a Salen-based COF, achieving both the formation of the COF structure and the functionalization with Salen moieties in a single step (Fig. 6).[152] This work paved the way for the development of a series of metallo-Salen-based COFs through post-synthetic metalation, broadening their applicability in catalysis and molecular adsorption. They synthesized the unique Salen-COF *via* the solvothermolysis of 1,3,5-tris[(5-*tert*-butyl-3-formyl-4-hydroxyphenyl)ethynyl]benzene and ethylenediamine, resulting in a highly crystalline material with a high Brunauer–Emmett–Teller (BET) surface area of 1366 $m^2 g^{-1}$. Post-synthetic metalation was performed using various metal ions, including Cu, Ni, Zn, Co, and Mn, yielding a family of M/Salen-COFs. Powder X-ray diffraction (PXRD) patterns confirmed that the crystalline structure of Salen-COF remained intact after metalation, demonstrating its structural robustness. These metallo-Salen-COFs have since been extensively investigated for catalytic applications, capitalizing on the diverse catalytic properties of the incorporated metal centers. Prior to this, in 2011, Nguyen and coworkers had reported a series of metallosalen-based MOFs containing Co, Zn, Cr, Cu, and Ni.[153]

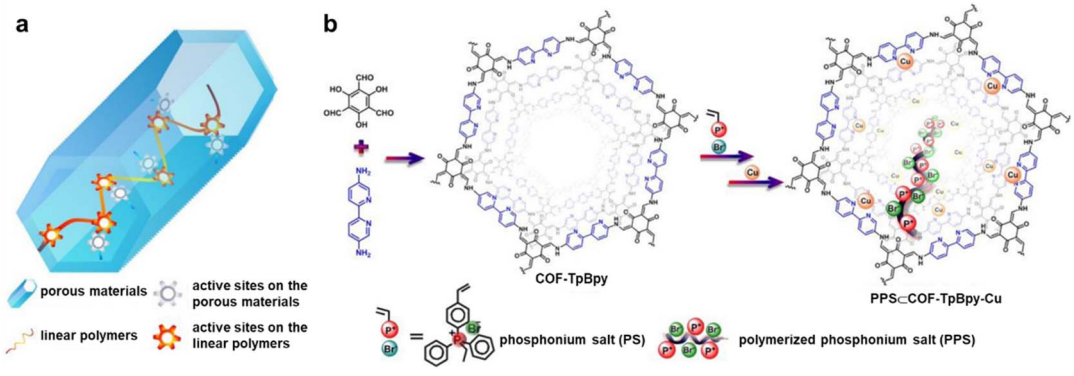

Fig. 5 (a) The concept of heterogeneous concerted catalysis involving active sites on porous materials and highly flexible linear polymers. (b) Schematic representation of PPS ⊂ COF-TpBpy-Cu synthesis, along with the structures of COF-TpBpy and PPS ⊂ COF-TpBpy-Cu. Reproduced with permission.[148] Copyright 2016, American Chemical Society.

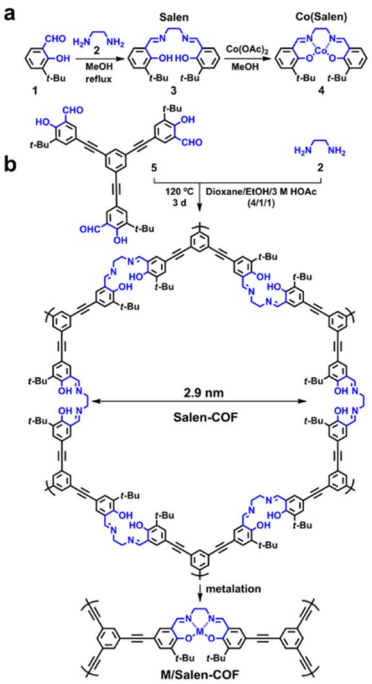

Fig. 6 (a) Classical synthesis of salen units and (b) one-step construction of salen-COF[a]. Reproduced with permission.[152] Copyright 2016, American Chemical Society.

They synthesized these frameworks by treating Mn^{III}SO-MOF, a Mn^{3+}(Salen)-based MOF, with H_2O_2 to remove the Mn^{3+} ions from the Salen struts. This process generated a vacant coordination environment within the framework, allowing for the subsequent introduction of various metal precursors to form isostructural MSO-MOF materials. This re-metalation strategy significantly expanded the functionality and tunability of Salen-based MOFs, offering a platform for diverse catalytic transformations and selective adsorption processes. These pioneering studies on both COFs and MOFs underscore the versatility of Salen linkers in framework materials, highlighting their potential in designing multifunctional porous materials for advanced applications in catalysis, separation, and sensing.

While functionality can be introduced into COFs or MOFs through coordination-based PSM, covalent PSM offers an alternative and widely adopted strategy for precisely modifying organic active sites on pore surfaces. This method is particularly valuable for fine-tuning the chemical environment within the frameworks, enabling enhanced control over their properties and functionalities. The concept of PSM in MOFs was first introduced by Cohen's group in 2007, marking a significant advancement in the field.[154] They demonstrated the covalent modification of the IRMOF-3 using acetic anhydride. IRMOF-3, featuring a cubic topology and amino-functionalized pore walls, was synthesized from $Zn(NO_3)_2 \cdot 4H_2O$ and 2-amino-1,4-benzenedicarboxylic acid (R_3-BDC). The free amino groups in IRMOF-3 provided a versatile platform for post-synthetic covalent modification. In a typical PSM reaction, crystals of IRMOF-3 were suspended in CH_2Cl_2 (or $CHCl_3$) and treated with pure acetic anhydride at room temperature, resulting in IRMOF-3-AM1, where the amino groups were converted to acetanilide groups. This pioneering study opened new possibilities for designing functionalized crystalline porous materials through post-synthetic modification strategies, allowing the precise tuning of chemical properties without disrupting the overall framework integrity. In the realm of COFs, Jiang's group successfully utilized PSM to functionalize COFs through click chemistry, employing azide-appended building units that reacted with various alkynes to yield triazole-functionalized COFs with tunable pore surface chemistry.[155] They synthesized *X*% N_3-COF-5 by combining 2,5-bis(azidomethyl)benzene-1,4-diboronic acid (N_3-BDBA), benzene-1,4-diboronic acid (BDBA), and hexahydroxytriphenylene (HHTP). The azide groups in the framework enabled further functionalization *via* 1,2,3-triazole rings through click reactions with alkynes, yielding *X*% RTrz-COF-5. By adjusting the proportion of azide units ($X = 5$, 25, 50, 75, and 100), they precisely controlled the density of functional groups, demonstrating a scalable strategy for surface engineering of COFs. Furthermore, the pore chemistry of these COFs was finely tuned by modifying the triazole moieties present on the pore walls.

Different triazole substitutions enabled precise control over the framework's binding affinity toward various gas molecules, enhancing their potential for efficient gas storage and selective gas separation. These modifications allowed COFs to be tailored for specific applications, such as the selective sorption of CO_2 over N_2. The advancements in PSM strategies for both MOFs and COFs underscore their versatility in functional material design. By leveraging covalent modifications, researchers can impart new properties to these frameworks, expanding their applications in catalysis, gas storage, molecular sieving, and sensing technologies. The ability to introduce and fine-tune functional groups post-synthetically provides a powerful tool for optimizing porous materials for targeted applications while preserving their inherent structural stability.

2.2.3 Host–guest-directed tuning of pore environments. Feng and Bu's research groups proposed the pore space partition (PSP) concept in MOFs and have reported a series of remarkable studies on utilizing sophisticated pore-partitioning agents to segment the 1D channels of MOFs into smaller pockets, thereby dramatically increasing the number of host–guest binding sites.[156,157] The key to their experimental success lies in the presence of OMSs in the framework, which facilitate the incorporation of pore-partitioning ligands. Currently, the most representative embodiment of the PSP concept is the partitioned-acs (pacs) platform, where fine and coarse adjustments to the building blocks have enabled the transformation of a prototype framework into an extensive and continuously expanding family of chemically robust materials.[158,159] These materials exhibit controllable pore metrics and functionalities, making them suitable for tailored applications. The compositional diversity of the pacs platform stems from its intrinsic multi-module nature, geometric flexibility, tolerance toward individual module variations, and the mutual structure-directing effects among various modules. Together, these factors enable the molecular-level uniform co-assembly of chemical components that are rarely seen together in other

systems. To achieve precise pore partitioning, they employed a strategy called symmetry-matching regulated ligand insertion, where a secondary ligand (L_s) is introduced into a primary framework. This approach leverages the symmetry and size matching between L_s and the geometrical arrangement of the framework's coordination sites as well as the channel dimensions. By incorporating a tripyridyl-type ligand into the synthesis of a MIL-88-type structure, they successfully developed a family of Ni-trimer-based MOFs (Fig. 7).[160] These materials significantly reduce the pore size of the parent MOF, leading to the newly synthesized CPM-33 family, which exhibits superior CO_2 uptake capacity. Notably, CPM-33b-Ni, in which all open metal sites are occupied, demonstrates CO_2 uptake capacity comparable to that of MOF-74 with the same metal (Ni) at 298 K and 1 bar.

The PSP strategy has also been applied to 2D COFs to subdivide their mesopores (2–50 nm) and micropores (1–2 nm) into ultramicropores (<1 nm). Two recent studies on pore partitioning in 2D COFs utilized aldehyde groups remaining in the channels of preformed COFs as anchoring sites, enabling amine-based insertions to partition the pore space into multiple smaller domains through post-synthetic Schiff-base reactions, achieving precise pore segmentation. Xu *et al.* employed a hexagonal boronic ester-linked COF, DBAAn-BTBA-COF, constructed from 1,3,5-benzenetriboronic acid (BTBA) and 4,4′-(2,3,6,7-tetrahydroxyanthracene-9,10-diyl)dibenzaldehyde (DBAAn), as the parent framework (Fig. 8).[161] This mesoporous COF features well-defined hexagonal pores with a diameter of 2.9 nm. The six aldehyde groups on each hexagonal unit, oriented toward the center of the 1D channels, were further reacted with a planar hexagonal amine-based building block possessing C_6 symmetry. This reaction formed imine bonds,

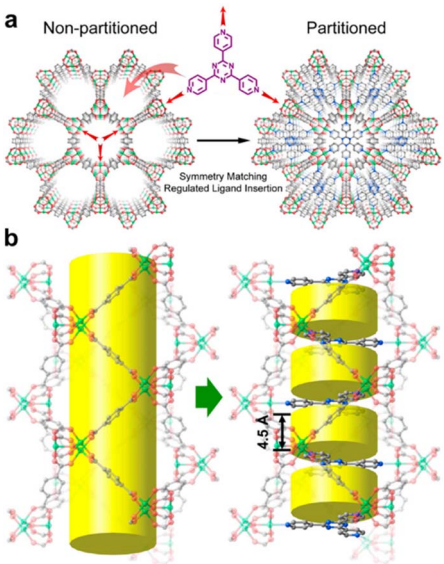

Fig. 7 Illustration of pore space partitioning *via* symmetry-matching regulated ligand insertion. (a) View along the *c*-axis and (b) side view of the channels, depicting the cylindrical channel before and after partitioning (green: Ni, red: O, blue: N, gray: C). Reproduced with permission.[160] Copyright 2015, American Chemical Society.

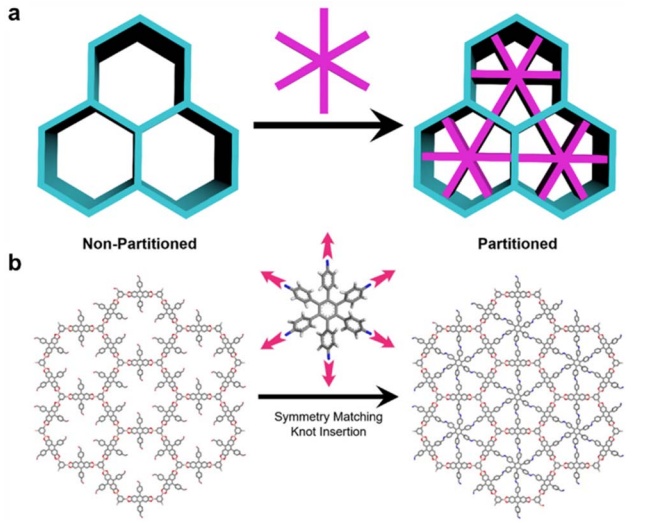

Fig. 8 (a) Graphical representation of pore partitioning in hexagonal channels. (b) Conversion of DBAAn-BTBA-COF into DBAAn-BTBA-HAPB-COF *via* symmetry-matching knot insertion. Reproduced with permission.[161] Copyright 2023, Springer Nature.

partitioning each pore into six equal domains. Hexaminophenyl benzene (HAPB) was identified as the optimal partitioning agent, yielding a new crystalline material, DBAAn-BTBA-HAPB-COF, where the original 2.9 nm pores were divided into six uniform ultramicropores of 6.5 Å. However, DBAAn-BTBA-HAPB-COF could not be synthesized *via* a one-pot procedure, underscoring the advantages of the post-synthetic PSP strategy in achieving precise pore size control. The resulting wedge-shaped ultramicroporous 1D channels endowed the COF with exceptional efficiency in separating five hexane isomers based on molecular sieving effects. Hao *et al.* extended this strategy to imine-linked 2D COFs, designing and synthesizing a series of tetragonal and hexagonal MTV-COFs with aldehyde groups anchored within their channels.[162] Additional linear or triangular linkers were then inserted into the center of the pore spaces, acting as partitioning agents to transform the micropores and mesopores into ultramicropores. Notably, the introduction of multi-N components into the partitioned COF 3-2P resulted in high I_2 and CH_3I uptake capacities of 0.42 and 0.24 g g^{-1} at 150 °C, respectively. These findings demonstrate that pore partitioning enables precise control over the pore environment and functionality of COFs, highlighting the significant potential of COF-based adsorbents for diverse applications.

Very recently, Zhang *et al.* reported a powerful and generalizable strategy for constructing metal-halide porous framework superlattices with spatially modulated chemical compositions within the pores of various MOFs.[163] By employing a one-pot synthesis approach, the authors achieved the confined growth of selected metal halides (PbI_2, $PbBr_2$, CdI_2, and $NiBr_2$) within a series of 3D Zr(IV)-based MOFs, resulting in the formation of highly ordered, single-crystalline porous superlattices. Critically, the local pore environments of the host MOFs—specifically, the cavity sizes, geometries, and spatial orientation of anchoring sites—played a key role in directing the

dimensionality (0D, 1D, or 2D) and structural arrangement of the metal-halide building units. This control arises from the influence of inter-node distances and spatial confinement on the nucleation and growth pathways of the halide crystals. Moreover, further treatment of these superlattices with selected amine molecules led to the formation of perovskite-like superlattices exhibiting highly tunable photoluminescence and chiroptical properties. This work highlights an innovative and versatile platform for engineering high-order, multi-dimensional single-crystalline superlattices with precisely tailored chemical functionality and emergent physical properties. The integration of inorganic components into MOF scaffolds in this manner not only provides a new avenue for pore regulation, but also opens up exciting possibilities for designing multifunctional hybrid materials for optoelectronic, chiral, and quantum applications.

3. Functional design and applications

With the versatile chemical tools available for tuning pore structures and chemistry in MOFs and COFs, their practical applications have been extensively explored over the past two decades. To obtain target materials with precise functionalities, the *de novo* synthetic strategy is an ideal approach, as it ensures a controlled degree of functional group incorporation at the ligand or monomer level. However, many desired framework materials with specific active sites cannot be directly synthesized through this method due to structural and synthetic limitations. As an alternative, PSM has emerged as a powerful strategy, allowing for the functionalization of organic backbones or metal clusters while preserving the integrity of the pristine framework and maintaining porosity. The ease of functionalizing pore surfaces in MOFs and COFs through sophisticated pore engineering has enabled the development of highly tailored materials for a wide range of practical applications. These materials have exhibited outstanding performance in gas storage and separation, heterogeneous catalysis, and environmental remediation, three key research areas in which we have conducted in-depth studies over the past decade. Through these efforts, we have proposed a series of innovative design and synthesis strategies for functionalizing MOFs and COFs, enabling the development of highly tailored materials with enhanced performance and expanded application potential. In the following discussion, we will highlight significant advancements in these fields, emphasizing how structural tuning and surface modifications in MOFs and COFs contribute to their superior functionalities and practical applications.

3.1 Gas storage/separation

MOFs and COFs, featuring uniform pore structures, large surface areas, tunable pore sizes, and customizable pore surface chemistry, have been extensively explored for gas storage and separation applications. Among these, MOFs have gained particular attention due to the efficiency of pore engineering in controlling pore structure and functionality, which significantly enhances their capability for differential molecular recognition. By precisely tailoring pore sizes, channel geometries, surface areas, and functional sites, novel MOF materials can be designed for highly selective.[164–168] Given the growing importance of clean energy,[169] considerable efforts have been dedicated to identifying materials for hydrogen storage,[170,171] methane storage,[172–174] and carbon dioxide capture.[175,176] The potential of MOFs in hydrogen storage was first demonstrated in 2003 when Yaghi's group reported MOF-5 as an H_2 adsorbent.[177] Since then, extensive research has led to the evaluation of hundreds of MOFs as physi-sorbents for hydrogen storage applications. It has been established that the gravimetric hydrogen storage capacities at 77 K and high pressures are strongly correlated with the pore volume and/or surface area of MOFs. For instance, an isoreticular series of MOFs with a rht topology, NOTT-112, NU-111, and NU-100 (also known as PCN-610), exhibits systematically increasing BET surface areas of 3800 $m^2\ g^{-1}$, ~5000 $m^2\ g^{-1}$, and 6143 $m^2\ g^{-1}$, respectively. Correspondingly, their total gravimetric hydrogen uptake at 77 K and 70 bar follows the same trend, with capacities of 10.0, 13.6, and 16.4 wt%, respectively.[178–181] This demonstrates the critical role of surface area and pore volume in optimizing hydrogen adsorption performance.

COFs have also been extensively investigated for hydrogen storage. Yaghi's group designed and synthesized a series of COFs tailored for H_2 adsorption.[182] Among them, COF-102 and COF-103 exhibit high BET surface areas of 3472 $m^2\ g^{-1}$ and 4210 $m^2\ g^{-1}$, respectively, while COF-108 stands out for its exceptionally low crystalline density of 0.17 $g\ cm^{-3}$. Theoretical predictions suggest that 3D COFs, such as COF-102, COF-103, COF-105, and COF-108, demonstrate 2.5 to 3 times higher hydrogen storage capacities compared to 2D COFs (*e.g.*, COF-1 and COF-5), primarily due to their greater surface areas and free volumes. Further computational studies on prototypical COFs predict that COF-105 could achieve an excess H_2 storage capacity of up to 10 wt% at 77 K and 80 bar, while COF-108 could reach similar capacities at 77 K and 100 bar. These values significantly surpass some well-known MOFs, such as MOF-177 (7.0 wt%)[183] and MOF-5 (7.1 wt%)[184] under similar conditions. In terms of volumetric storage, COF-102 demonstrated a maximum excess H_2 uptake of 40.4 $g\ L^{-1}$ at 100 bar, highlighting its potential as a highly efficient hydrogen storage material. To further enhance hydrogen adsorption in COFs, Pramudya *et al.* proposed a strategy involving the chelation of transition metals (TMs) inside 3D COFs, utilizing various linker sites to host metal ions and improve H_2 binding energies (Fig. 9).[185] Computational studies revealed that first-row transition metals (Sc to Cu) could achieve interaction strengths comparable to, or even surpassing, those of precious late transition metals (Pd and Pt). This finding suggests that it is unnecessary to rely on expensive and heavy transition metals to achieve strong H_2 binding. Beyond COFs, lightweight non-transition metal ions, such as Li^+, incorporated *via* ion exchange into anionic coordination MOFs, have also been explored to enhance hydrogen adsorption performance. A series of Li^+-exchanged anionic In-diisophthalate frameworks (NOTT-200, NOTT-206, and NOTT-208) demonstrated simultaneous increases in both hydrogen uptake capacity and adsorption

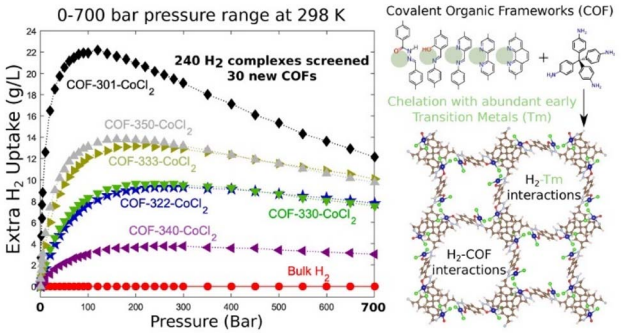

Fig. 9 Design principles for high H_2 storage through chelation of abundant transition metals in covalent organic frameworks under 0–700 bar at 298 K. Reproduced with permission.[185] Copyright 2016, American Chemical Society.

enthalpy, offering a promising approach for optimizing H_2 storage in porous materials.[186]

Beyond hydrogen storage, MOFs and COFs have also demonstrated remarkable efficiency in methane storage, offering a promising alternative for natural gas storage and transportation. Their tunable pore structures enable strong methane adsorption at moderate pressures, addressing key challenges in gas delivery systems. Additionally, both MOFs and COFs have been widely explored for CO_2 capture, benefiting from their highly selective adsorption sites, which can be chemically functionalized to enhance CO_2 affinity while minimizing energy-intensive regeneration processes. In the case of methane storage, the incorporation of specific functional sites in MOFs can significantly enhance CH_4 uptake by increasing interactions with methane molecules. One effective strategy involves introducing OMSs into the framework to improve CH_4 affinity. For instance, HKUST-1, featuring well-suited pore cavities and abundant accessible Cu sites, exhibits an exceptional CH_4 volumetric uptake of 267 cm^3 (STP) cm^{-3} at room temperature and 65 bar, where STP is standard temperature and pressure.[187] This makes HKUST-1 the first MOF material with the potential to meet the U.S. Department of Energy (DOE) targets for volumetric CH_4 uptake. Further advancements in MOF design have led to even greater methane storage capacities. Chen and coworkers developed a novel NbO-type porous MOF, UTSA-76a, incorporating pyrimidine groups and OMSs, which demonstrated an outstanding methane storage capacity of 257 cm^3 (STP) cm^{-3} at 298 K and 65 bar.[188] Moreover, UTSA-76a surpassed HKUST-1 in methane storage performance, exhibiting a higher working capacity of 197 cm^3 (STP) cm^{-3} and a storage density of 0.263 g g^{-1}. This superior performance is attributed to the extensive rotational freedom of its central "dynamic" pyrimidine cluster, which optimizes CH_4 packing under high-pressure conditions.

Recently, Yin *et al.* developed two isostructural 3D COFs featuring a rare self-catenated alb-3,6-Ccc2 topology with a pore size of 1.1 nm.[189] Utilizing a [6 + 3] topology design strategy, the authors constructed highly porous 3D COFs by selecting 1,3,5-trimethyl-2,4,6-tri[3,5-di(4-aminophenyl-1-yl)phenyl-1-yl] benzene (TAPB-Me) and its analog 1,3,5-triethyl-2,4,6-tri[3,5-di(4-aminophenyl-1-yl)phenyl-1-yl]benzene (TAPB-Et) as 6-connected polyhedral nodes, while 1,3,5-triformylbenzene (TFB) served as the 3-connected building block, yielding 3D-TFB-COF-Me and 3D-TFB-COF-Et, respectively. Both COFs exhibited exceptionally high BET surface areas exceeding 4000 m^2 g^{-1}, ranking among the highest reported for imine-linked COFs and placing them in the top tier of all known microporous materials. Given their high surface areas and microporous architectures, their high-pressure CH_4 adsorption performance was evaluated up to 100 bar at 298 K. The gravimetric methane uptake values for 3D-TFB-COF-Me and 3D-TFB-COF-Et reached 423 mg g^{-1} and 429 mg g^{-1}, respectively. Based on their crystal densities, their volumetric methane uptakes were measured at 249 cm^3 (STP) cm^{-3} and 264 cm^3 (STP) cm^{-3}, with 3D-TFB-COF-Et surpassing the latest DOE CH_4 storage target of 263 cm^3 (STP) cm^{-3} at 298 K and 100 bar. These findings further underscore the significant potential of MOFs and COFs in methane storage applications, with ongoing research directed toward enhancing adsorption capacities through pore engineering and functional site modifications.

Beyond gas storage, MOFs have demonstrated exceptional potential for gas separations, leveraging their precisely tunable pore structures and surface chemistry. These materials have been widely investigated for key industrial separations, including ethylene/ethane (C_2H_4/C_2H_6), propylene/propane (C_3H_6/C_3H_8), acetylene/ethylene (C_2H_2/C_2H_4), acetylene/carbon dioxide (C_2H_2/CO_2), propyne/propylene (C_3H_4/C_3H_6), C_4 hydrocarbon separations, C_6/C_8 isomer separation, CO_2 capture and separation.[190–192] Chen's group pioneered the application of microporous MOFs in industrial gas separation, demonstrating their separation performance and efficiency through fixed-bed adsorption and breakthrough experiments.[193–195] As early as 2005, Chen and Dai first reported the use of microporous MOFs for alkane isomer separation.[196] MOF-508, synthesized from H_2BDC, 4,4′-bipyridine (Bipy), and $Zn(NO_3)_2 \cdot 6H_2O$, was employed as a gas-chromatographic (GC) filler, successfully separating linear and branched isomers of pentane and hexane. MOF-508, a double-interpenetrated MOF, consists of 6-connected paddle-wheel zinc clusters bridged by bdc^{2-} and Bipy linkers, forming a three-dimensional framework with pcu topology. Its one-dimensional channels (~4.0 Å in diameter) selectively accommodate linear alkanes while excluding branched isomers, demonstrating the size-exclusion effect. Furthermore, MOF pore sizes can be rationally tuned by adjusting their degree of interpenetration, as exemplified by the non-interpenetrated microporous MOF $[Zn_2(bdc)_2(dabco)]$ (dabco = 1,4-diazabicyclo[2,2,2]octane), which exhibits a similar pcu topology but with optimized pore accessibility.[197] In 2016, Chen and co-workers conducted a comprehensive study on acetylene (C_2H_2) and ethylene (C_2H_4) adsorption using a series of SIFSIX materials, including SIFSIX-1-Cu, SIFSIX-2-Cu, SIFSIX-2-Cu-i, SIFSIX-3-Cu, SIFSIX-3-Zn, and SIFSIX-3-Ni.[198] By finely tuning the pore chemistry and size, all of these materials exhibited higher C_2H_2 uptake than C_2H_4, demonstrating selective acetylene adsorption. Notably, SIFSIX-2-Cu-i displayed an exceptionally high C_2H_2 adsorption capacity (2.1 mmol g^{-1} at 298 K and 0.025 bar), with a C_2H_2/C_2H_4 selectivity of 39.7–44.8,

effectively overcoming the typical trade-off between C_2H_2 selectivity and uptake capacity. Chen and co-workers further extended their research into C_2H_2/CO_2 separation by designing MOFs with enhanced selectivity. A notable example is UTSA-74, an isomeric Zn-MOF-74, with the formula $Zn_2(H_2O)(dobdc)\cdot 0.5(H_2O)$.[199] UTSA-74 exhibits comparable C_2H_2 adsorption capacity (145 $cm^3\ cm^{-3}$) to Zn-MOF-74 but significantly lower CO_2 uptake (90 $cm^3\ cm^{-3}$) due to differences in Zn_2 coordination environments. Unlike Zn-MOF-74, where Zn_2 sites are terminally bound to CO_2, in UTSA-74, the Zn_2 sites are bridged by CO_2 molecules, reducing CO_2 binding strength and resulting in a high C_2H_2/CO_2 selectivity of 9 at 100 kPa and 298 K. These findings highlight the remarkable adaptability of MOFs for gas separations, with ongoing research focusing on pore size control, functionalization, and metal-site engineering to optimize selectivity and adsorption capacity for industrial applications.

Our group has recently developed a series of microporous MOFs featuring gas-specific nanotraps for the efficient capture and separation of key industrial gases. In early 2021, we introduced an ultra-strong C_2H_2 nanotrap designed to selectively capture acetylene and separate C_2H_2/CO_2 mixtures (Fig. 10a).[200] This was achieved using the alkyl-functionalized MOF ATC-Cu, which possesses uniquely positioned, oppositely adjacent Cu paddlewheel open metal sites, significantly enhancing its affinity for acetylene molecules. ATC-Cu was synthesized *via* a hydrothermal reaction between 1,3,5,7-adamantane tetracarboxylic acid (H_4ATC) and copper nitrate hydrate, forming a robust 4,4-coordinated network where four Cu paddlewheels are linked by ATC ligands. The exceptionally short Cu–Cu distance of 4.43 Å (after subtracting van der Waals radii) creates a dual potential coordination site, enabling strong C_2H_2 binding. Additionally, the aliphatic hydrocarbon cavities in ATC-Cu contain twelve inward-facing hydrogen atoms positioned at an average distance of 3.5 Å from the cavity center, providing additional adsorption sites for C_2H_2. The synergistic effect of these structural features results in an unprecedented acetylene binding affinity, as demonstrated by a record-high isosteric heat of adsorption (Q_{ST} = 79.1 kJ mol^{-1}). ATC-Cu exhibited the highest reported pure C_2H_2 uptake at 1×10^{-2} bar and remarkable selectivity in a binary equimolar C_2H_2/CO_2 mixture at 298 K and 1 bar, setting a new benchmark for C_2H_2 capture and separation. Following this, we developed a MOF-based hydrogen-bonding nanotrap strategy to further enhance acetylene storage and separation (Fig. 10b).[201] By introducing hydrogen-bonding acceptor sites on the pore surface, we optimized the separation of C_2H_2/CO_2 mixtures across three isostructural MOFs: MIL-160, CAU-10H, and CAU-23. Among them, MIL-160, synthesized from 2,5-furandicarboxylic acid and $Al(OH)(CH_3COO)_2$, demonstrated exceptional C_2H_2 storage capacity (191 $cm^3\ g^{-1}$, or 213 $cm^3\ cm^{-3}$) while maintaining a significantly lower CO_2 uptake (90 $cm^3\ g^{-1}$) under ambient conditions, highlighting its superior C_2H_2 selectivity.

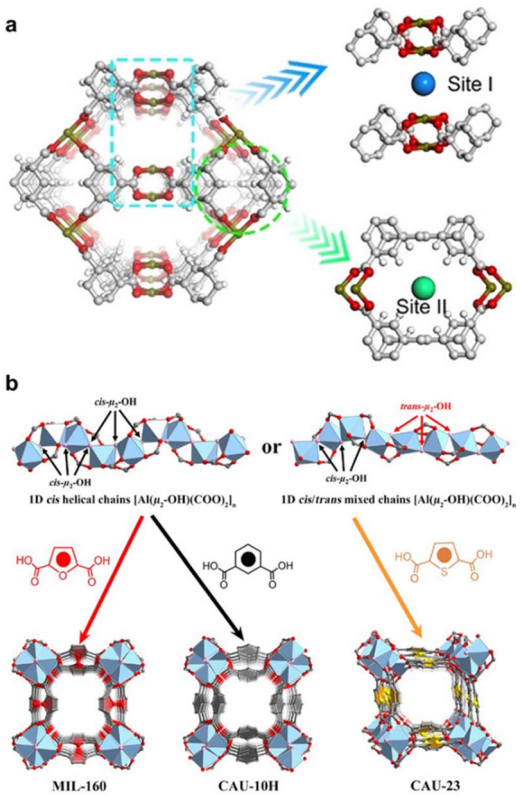

Fig. 10 (a) The channel structure of ATC-Cu and the two primary C_2H_2 binding sites within the framework. Reproduced with permission.[200] Copyright 2021, American Chemical Society. (b) 1D chains $[Al(\mu_2\text{-}OH)(COO)_2]_n$ and V-shaped ligands (H_2FDC, *m*-H_2BDC, and H_2TDC) assemble into three isostructural 3D frameworks of MIL-160, CAU-10H, and CAU-23, respectively. Hydrogen atoms are omitted for clarity. Color code, Al: pale blue; O, red and rose; C, 50% gray. Reproduced with permission.[201] Copyright 2021, American Chemical Society.

To further refine gas separation performance, we implemented a dynamic spacer installation (DSI) strategy to construct a series of multifunctional MOFs (LIFM-61/31/62/63) with optimized pore spaces and environments for ethane/ethylene separation.[202] These MOFs were derived from the prototype LIFM-28, with pore volumes expanded (from 0.41 to 0.82 $cm^3\ g^{-1}$) and pore sizes reduced (from 11.1 × 11.1 $Å^2$ to 5.6 × 5.6 $Å^2$) by incorporating linear dicarboxylic acids into the replaceable coordination sites. Among them, LIFM-63, post-synthetically modified with biphenyl-4,4′-dicarboxylic acid (H_2BPDC) and 2′-methyl-[1,1′:4′,1′-terphenyl]-4,4″-dicarboxylic acid (H_2MTPDC), exhibited exceptional C_2H_6 uptake and C_2H_6/C_2H_4 selectivity. This was attributed to enhanced C–H···F and C–H···π interactions enabled by its optimized pore volume, small pore size, and tailored pore surface chemistry. LIFM-63 demonstrated a remarkable ethane adsorption capacity (4.8 mmol g^{-1}), nearly three times higher than its prototypical counterpart (1.7 mmol g^{-1}) at 273 K and 1 bar. Additionally, we explored the impact of pore functionalization on gas separation by synthesizing two isostructural Ni-based MOFs, [Ni(btz)Cl]·Cl (Ni-MOF-1) and [Ni(bdp)] (Ni-MOF-2), using organic linkers with rich aromatic moieties: btz(1,4′-bis(4*H*-1,2,4-triazol-4-yl)benzene) and bdp(1,4-benzenedipyrazole), respectively.[203] In Ni-MOF-1, the presence of Cl^- ions partially obstructed the pore spaces and weakened C–H···π interactions, leading to negligible C_2H_6/

C_2H_4 separation capability. In contrast, Ni-MOF-2, with open pore spaces and fully accessible aromatic rings, exhibited multiple and stronger C–H···π interactions favoring C_2H_6 adsorption over C_2H_4. As a result, Ni-MOF-2 demonstrated exceptional ethane/ethylene separation performance, ranking among the best porous materials for this critical industrial gas separation process. These studies collectively underscore the power of rational MOF design and pore engineering in achieving precise gas capture and separation, paving the way for advanced materials tailored for industrial applications.

Due to their typically larger pore sizes (>1 nm) than MOFs, most unmodified 2D COFs are not well-suited for gas separation, as the lack of tight molecular sieving limits their selectivity. However, certain 3D COFs have demonstrated promising potential in hydrocarbon separation. For instance, McGrier and co-workers synthesized and metalated a 3D COF containing π-electron conjugated dehydrobenzoannulene (DBA), yielding Ni-DBA-3D-COF *via* metalation of the pristine DBA-3D-COF.[29] The metalation process resulted in only a slight reduction in BET surface area, from 5083 $m^2\ g^{-1}$ to 4763 $m^2\ g^{-1}$, preserving the material's high porosity. The ethane/ethylene separation performance of Ni-DBA-3D-COF was assessed through gas adsorption isotherms at 273 K and 295 K over a pressure range of 0 to 1.2 bar, revealing a moderate enhancement in adsorption capacity, with an increase of 0.07 mmol for ethane and 0.13 mmol for ethylene at 295 K. Although the enhancement was modest, this proof-of-concept study highlights the feasibility of utilizing metalated COFs for hydrocarbon separations and paves the way for further optimization. Beyond hydrocarbon separations, COFs have also been explored for precise gas separation at the molecular level. Fan *et al.* introduced an ultramicropore-in-nanopore concept, employing a matryoshka-like pore-channel engineering strategy to achieve angstrom-level control over COF channel sizes.[204] This was accomplished *via in situ* encapsulation of α-cyclodextrin (α-CD) within the 1D nanochannels of a COF membrane during interfacial polymerization. The resulting LA-α-CD-in-TpPa-1 membrane demonstrated exceptional H_2 separation performance, exhibiting a high H_2 permeance (~3000 GPU) along with significantly enhanced selectivity (>30) for H_2 over CO_2 and CH_4. This enhancement was attributed to the formation of fast and selective H_2 transport pathways, showcasing a novel approach for precisely tuning COF pore structures for advanced gas separation applications. These studies underscore the growing versatility of COFs in gas separation, particularly through pore chemistry and pore size engineering, which open up new possibilities for designing highly selective, high-performance separation membranes or adsorbents.

3.2 Catalysis

COFs and MOFs have emerged as highly promising materials for heterogeneous catalysis due to their high surface area, tunable pore structures, and versatile active sites. Through pore engineering, the size, shape, and surface chemistry of their pores can be precisely tailored to enhance substrate diffusion, reactant accessibility, and selectivity, making them highly efficient catalytic platforms. MOFs, with metal nodes, provide Lewis acid sites that facilitate oxidation, hydrogenation, and C–C coupling reactions. In contrast, COFs, composed of fully organic linkages, can be designed with catalytically active sites through the incorporation of specific functional groups or by coordinating with metal species, enabling diverse catalytic applications. Both materials allow PSM, including metalation, ligand engineering, and biomimetic site incorporation, further enhancing catalytic efficiency. The π-conjugated backbones of COFs make them ideal for photocatalysis and electrocatalysis, enabling applications in CO_2 reduction and water splitting. Additionally, their excellent chemical and thermal stability ensures long-term catalytic performance with easy recovery and recyclability, making them superior to many homogeneous catalysts. By leveraging precise pore engineering, researchers have designed MOFs and COFs with hierarchical porosity, OMSs, and functionalized channels, optimizing catalytic activity for oxidation, hydrogenation, cross-coupling, photocatalysis, and electrocatalysis.

During the synthesis of MOF materials, solvents often participate in coordinating with central metal nodes. These solvents can be completely or partially removed by subjecting the MOFs to high temperatures under vacuum or other controlled conditions, exposing unsaturated metal sites that serve as Lewis acid sites for multiphase catalytic applications. To further enhance catalytic performance, our group developed a feasible strategy to incorporate linear ionic polymers within MOF pores *via in situ* free radical polymerization of monomer salts, creating synergistic catalytic sites within a single material.[205] A well-known MOF, MIL-101,[206] synthesized from $Cr(NO_3)_3 \cdot 9H_2O$ and terephthalic acid under solvothermal conditions, was treated with ethanol to remove the trapped DMF molecules within its pores. Subsequently, MIL-101 was mixed with a monomer salt, 3-ethyl-1-vinyl-1*H*-imidazol-3-ium bromide, in DMF and stirred at room temperature, allowing the monomer to settle inside the MOF pores, ensuring successful *in situ* polymerization of the ionic polymer. MIL-101, featuring mesoporous cages, high stability, and open chromium(III) metal sites, provides abundant accessible Lewis acid sites ideal for hosting flexible catalytic sites and acting as a co-catalyst. The resulting material, MIL-101-IP, was evaluated for CO_2 fixation and the transformation of various epoxides into cyclic carbonates. By integrating OMSs inside rigid MOF frameworks and introducing halide ions *via* immobilized ionic polymers, the unification of two catalytically active components was achieved, demonstrating that pore chemistry can be readily tailored through a host–guest strategy. This highlights the potential of engineering synergistic catalytic systems within porous materials for a wide range of applications.

Heterometallic MOFs have also demonstrated superior catalytic performance compared to their single-metallic counterparts due to their enhanced chemical stability and tunable pore chemistry, which can be precisely controlled by adjusting the metal ratios within the framework. Fu *et al.* developed a double-metallic MOF-74 (Cu/Co) with various Cu/Co ratios *via* a facile one-pot synthesis method, ensuring a uniform distribution of Cu^{2+} and Co^{2+} throughout the structure.[207] By carefully

tuning the Cu/Co ratio, not only was the oxidation activity modulated, but the selectivity of oxidation products was also finely controlled. Furthermore, the incorporation of secondary metal ions or clusters in heterometallic MOFs can regulate the electronic properties of active sites, significantly enhancing electrocatalysis and photocatalysis performance. Using a similar method, Tang and co-workers synthesized ultrathin bimetal-organic framework nanosheets (NiCo-UMOFNs) using a mixed solution of Ni^{2+}, Co^{2+}, and benzenedicarboxylic acid (BDC).[208] The resulting UMOFNs exhibited nanometer-scale thicknesses, enabling rapid mass transport and superior electron transfer, along with a high percentage of exposed catalytically active surfaces containing coordinatively unsaturated metal sites, ensuring exceptional catalytic activity. Additionally, the distinct surface atomic structures and bonding arrangements of NiCo-UMOFNs could be readily identified and tuned. Electron transfer from Ni to Co clusters resulted in optimized electronic states, significantly improving the electrochemical oxygen evolution reaction (OER) activity compared to monometallic Co-UMOFNs, Ni-UMOFNs, and bulk NiCo-MOFs. The metal ions/clusters can also be manipulated by PSM, Cohen and co-workers prepared UiO-66-NH_2(Zr/Ti) catalysts through post-synthetic method, whose electron accepting levels were lowered by the Ti doping, which can be readily achieved by post-synthetic ion exchange of UiO-66-NH_2(Zr) with $TiCl_4(THF)_2$ in DMF solution (Fig. 11).[209] The newly modified UiO-66-NH_2(Zr/Ti) showed higher CO_2 photoreduction activity and HCOOH selectivity (5.8 mmol mol^{-1}), 1.7 times higher than the monometallic UiO-66-NH_2(Zr).

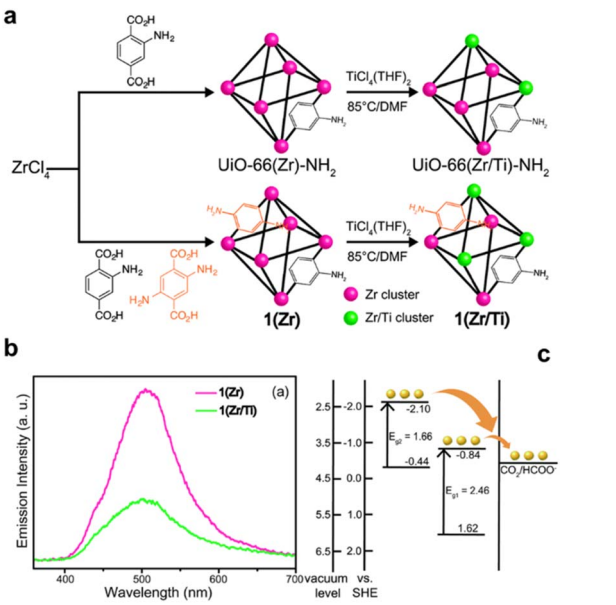

Fig. 11 (a) Synthesis of mixed-ligand MOF 1(Zr) *via* PSE to obtain mixed-metal MOFs 1(Zr/Ti) and UiO-66(Zr/Ti)-NH_2. (b) Photoluminescence spectra of 1(Zr) and 1(Zr/Ti). (c) Energy band structure of 1(Zr/Ti) derived from UPS and F(R) results, showing that heterogeneous ligands create two energy levels within the MOF, potentially facilitating CO_2 catalysis. Reproduced with permission.[209] Copyright 2015, Royal Society of Chemistry.

Jiang's group has been at the forefront of developing MOFs with precise pore engineering to enhance catalytic performance across multiple reactions.[210–212] Recently, they introduced a simple yet effective strategy to regulate the spin states of catalytic Co centers by altering their coordination environments. Through post-synthetic metal exchange, Co species were incorporated into a stable Zn-based MOF, yielding three distinct active sites, Co–OAc, Co–Br, and Co–CN, within the MOF pores for CO_2 photoreduction (Fig. 12).[213] By changing the Co precursor, Co centers coordinated with $-CH_3COO$, –Br, or –CN, precisely tuning their coordination environment and spin states. Experiments and theory showed that this spin-state modulation—without changing Co's oxidation state—greatly enhanced charge separation, CO_2 adsorption, and activation. Among the three variants, Co–OAc, which exhibited the highest spin state, demonstrated superior charge separation and optimized energy barriers for CO_2 adsorption and activation, resulting in an outstanding photocatalytic CO_2 reduction rate of 2325.7 μmol g^{-1} h^{-1} with 99.1% selectivity toward CO. To further explore MOFs as hosts for catalytically active species, Jiang's group employed UiO-66 as a template to encapsulate metal nanoparticles (NPs) and nanoclusters (NCs) within its pore cages. While NCs with atomically precise structures hold great promise for catalysis, their tendency to aggregate and the spatial resistance of surface ligands pose significant challenges. The spatial confinement effect of MOFs provides an ideal protective environment to address these issues. In their studies, Au_{25} NCs[214] and a series of MAg_{24} (M = Ag, Pd, Pt, and Au) NCs[215] were successfully encapsulated into UiO-66-X, forming Au_{25}@UiO-66-X (X = H, NH_2, OH, and NO_2) and MAg_{24}@UiO-66-NH_2. These composites allowed for precise tuning of electron density and substrate adsorption properties through variations in both the encapsulated NCs and the MOF ligands. Additionally, various NPs, including Pt NPs and PdCu NPs, were incorporated into MOFs for enhanced catalytic applications. For example, Jiang's group synthesized UiO-66-SO_3H ($Zr_6O_4(OH)_4$(-BDC-SO_3H)$_6$, denoted as UiO-S) to host PdCu NPs *via* PSM.[216] To further optimize its catalytic properties, a hydrophobic polydimethylsiloxane (PDMS) coating was introduced, yielding a composite catalyst denoted as PdCu@UiO-S@PDMS. The electron transfer within PdCu NPs facilitated N_2 activation,

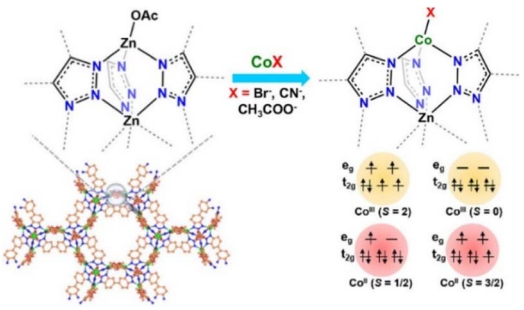

Fig. 12 Synthesis of Co–OAc, Co–Br, and Co–CN with different spin states of Co^{II} and Co^{III} *via* a postsynthetic exchange strategy. Reproduced with permission.[213] Copyright 2024, American Chemical Society.

while the protonated sulfonic acid groups provided an essential proton source for nitrogen reduction reaction (NRR). Meanwhile, the PDMS coating selectively suppressed water contact with PdCu while still allowing the sulfonate ($-SO_3^-$) groups to extract protons from water. This unique microenvironment efficiently supplied protons while suppressing the competitive hydrogen evolution reaction (HER), resulting in an optimized system for electrocatalytic NRR with enhanced performance. Expanding on this work, Jiang's group further engineered MOF-based core–shell structures to fine-tune catalytic activity.[217] By varying the functional groups of MOF ligands, they designed a set of UiO-66-X (X = –H, –Br, –NA (naphthalene), $-OCH_3$, –Cl, $-NO_2$) shells coated onto UiO-66-NH_2@Pt, forming UiO-66-NH_2@Pt@UiO-66-X. These core–shell MOF composites enabled simultaneous modulation of both the microenvironment around the Pt active sites and the photosensitive UiO-66-NH_2 core. This precise structural control significantly influenced the photocatalytic H_2 production performance. Among the various functionalized composites, UiO-66-NH_2@Pt@UiO-66-H exhibited the highest H_2 production rate of 2708.2 μmol g^{-1} h^{-1}, approximately 222 times higher than that of UiO-66-NH_2@Pt@UiO-66-NO_2. Their pioneering work has opened new avenues for designing supported catalysts with precisely tailored pore chemistry, demonstrating the immense potential of MOF-based materials for advanced catalytic applications.

Our group was the first to report the grafting of frustrated Lewis pairs (FLPs) into the pore space of MOFs by tailoring the pore environment.[218] MIL-101 (Cr) was selected as the platform to host FLPs due to its exposed Cr^{III} open sites in the secondary building unit (Fig. 13a).[219] One site serves as an anchor for the FLP, while the other, along with the hydroxyl group residing at the third Cr^{III} site, preferentially interacts with the targeted double bond in the substrate to facilitate its activation. In this work, the FLP, $B(C_6F_5)_2$(Mes)/DABCO, was successfully anchored into MIL-101(Cr), yielding MIL-101(Cr)-FLP. This catalyst demonstrated the selective hydrogenation of imine bonds in α,β-unsaturated imine compounds to produce unsaturated amine compounds using H_2 gas at room temperature, while this transformation is not achievable with FLPs in a homogeneous system. This represents the first example of an FLP-based heterogeneous catalyst capable of selectively hydrogenating α,β-unsaturated organic compounds, thereby paving the way for the development of precious-metal-free chemoselective heterogeneous catalysts. Building on this breakthrough, our group and co-workers explored various combinations of FLPs and MOFs to investigate their catalytic performance. A novel P/B-type FLP containing a phosphorus-based Lewis base was synthesized within the MOF NU-1000, demonstrating high efficiency in the selective hydrogenation of quinoline and indole to yield tetrahydroquinoline and indoline-type drug compounds with excellent yield and recyclability (Fig. 13b).[220] Additionally, chiral FLPs (CFLPs) derived from $RB(C_6F_5)_2$ (R = C_6F_5 or C_9H_{11}) and various chiral Lewis bases were synthesized and anchored into MOFs, resulting in CFLP@MIL-101(Cr)[221] and EMR@MOF,[222] respectively. These MOFs exhibited efficient heterogeneous asymmetric hydrogenation with excellent recyclability and regenerability,

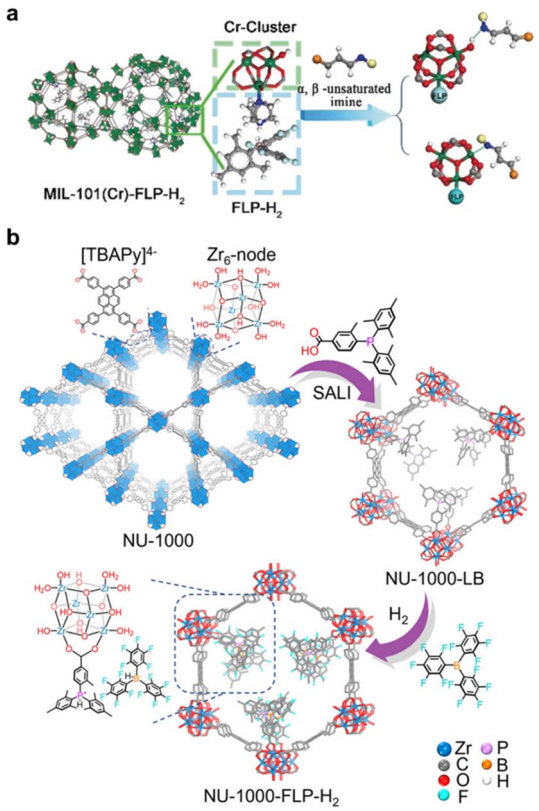

Fig. 13 (a) The "activation" process involving a $Cr_3(\mu_3\text{-O})(COO)_6(OH)(H_2O)_2$ cluster in MIL-101(Cr)-FLP-H_2. Reproduced with permission.[219] Copyright 2019, John Wiley and Sons. (b) Construction pathway of NU-1000-FLP-H_2. Reproduced with permission.[220] Copyright 2023, American Chemical Society.

establishing CFLP@MOF as a promising platform for asymmetric catalysis. This approach bridges different fields of chemistry to address challenges in asymmetric catalysis and beyond.

Following these advancements, our group realized a set of metal-free chiral frustrated Lewis pair frameworks within COFs as well. We proposed a general strategy for integrating rationally designed crystalline COFs with newly developed CFLPs to create chiral frustrated Lewis pair frameworks (CFLPFs).[223] COF-TAPB-3P-COOH was first synthesized using 1,3,5-tris(4-aminophenyl) benzene (TPB) and *p*-terphenyl-2′,5′-dicarboxylic acid-4,4″-dicarboxaldehyde (3P-COOH). Through covalent post-synthetic modification, chiral *N*1,*N*1-di-*tert*-butyl-3,3-dimethylbutane-1,2-diamine ($R1NH_2$) and chiral 4,5-dihydro-4-phenyl-2-oxazolemethanol (R2OH) were introduced as chiral Lewis bases, yielding COF-TAPB-3P-COHNR1* and COF-TAPB-3P-COOR2*, respectively, which were further associated with $B(C_6F_5)_3$ to form CFLPF1 and CFLPF2. Both metal-free CFLPFs exhibited superior activity and enantioselectivity for asymmetric olefin hydrogenation, along with outstanding stability and recyclability.

Our group has also developed various strategies to tune pore geometry and active sites in COFs to optimize inner pore chemistry and catalytic performance.[224–226] Due to their purely organic skeletons, large pore sizes, high chemical stability, and

easy recyclability, COFs have emerged as a promising platform for hosting biocatalysts, such as enzymes, to overcome challenges in cell-free enzyme catalysis. COFs provide robust protection against enzyme deactivation, enhance recyclability, and improve operational stability. In a study published in 2017, our group selected TPB-DMTP-COF (COF-OMe), synthesized by the condensation of dimethoxyterephthaldehyde (DMTP) and TPB, as a host material due to its exceptional stability, high surface area, and ordered one-dimensional (1D) channel-like pores (3.3 nm) (Fig. 14).[225] Lipase PS (3.0 nm × 3.2 nm × 6.0 nm) was immobilized into COF-OMe in a phosphate buffer solution, yielding lipase@COF-OMe with a high enzyme uptake capacity of 0.95 mg mg^{-1}. Recognizing that protein migration into porous materials is driven by surface interactions, we investigated the impact of pore environments on enzyme loading. Three isoreticular COFs (COF-V, COF-OH, and COF-ONa) with varying degrees of hydrophilicity were synthesized for comparison. COF-V was obtained from 2,5-divinylterephthalaldehyde and TPB, COF-OH from 2,5-dihydroxyterephthalaldehyde and TPB, and COF-ONa by treating COF-OH with NaOH. Under identical conditions, COF-Vexhibited a slightly lower lipase PS uptake (0.78 mg mg^{-1}) than COF-OMe, likely due to its reduced surface area. COF-OH and COF-ONa displayed even lower uptake capacities (0.75 and 0.59 mg mg^{-1}, respectively), supporting the hypothesis that a hydrophobic pore environment favors enzyme infiltration. Beyond surface properties, pore structure also plays a crucial role in enzyme immobilization. To verify this, we synthesized an amorphous analogue (POP-OMe) of COF-OMe using the same monomers but in DMSO as the solvent. POP-OMe exhibited a significantly lower BET surface area (1740 m^2 g^{-1} *vs.* 1056 m^2 g^{-1} for COF-OMe) and a reduced enzyme uptake (0.58 mg mg^{-1}), achieving only 65% of COF-OMe's performance. Subsequent studies focused on tuning pore heterogeneity in COFs to enhance enzyme accessibility and resistance to denaturants.[226] COFs with dual pores were designed and synthesized to improve enzyme immobilization. The dual-pore structure of COF-ETTA-EDDA was confirmed by DFT pore size distribution analysis, revealing micropores (~13.9 Å) and mesopores (~38.5 Å). The larger mesopores facilitated enzyme immobilization, while the smaller micropores remained unoccupied, serving as transport channels for substrates and products. This structural optimization effectively reduced diffusion path lengths and significantly enhanced flux rates, thereby improving mass transport within the material. As a result, it established clear structure–property design rules for creating hierarchical pore architectures, which are crucial for optimizing enzyme-encapsulation applications and improving catalytic efficiency.

3.3 Environmental remediation

Given their high surface area, well-defined pore structures, and versatile functionalization potential, MOFs and COFs have gained significant attention as promising materials for environmental remediation. They demonstrate great potential for the binding and extraction of various pollutants, offering innovative solutions to pressing environmental challenges, including water purification, air pollution control, and toxic waste treatment. Task-specific binding sites can be incorporated into MOFs and COFs through *de novo* synthesis or post-synthetic modification, enabling the introduction of complexing functionalities to effectively capture and neutralize diverse contaminants.

Among the various environmental concerns, the adsorption of organic dyes and heavy metals from water has long been a major focus, and MOFs and COFs have been extensively studied for their effectiveness in removing these pollutants from water supplies. One notable example of an environmentally friendly MOF is MOF-235(Fe), a structural analog of the well-known MIL-101, both synthesized from $FeCl_3 \cdot 6H_2O$ and BDC, but differing in crystal structures.[227] Despite being classified as a nonporous or low-porosity MOF, MOF-235(Fe) has demonstrated strong adsorption capabilities for both anionic (*e.g.*, methyl orange, MO) and cationic (*e.g.*, methylene blue, MB) dyes in aqueous solutions.[228] Additionally, the presence of Fe^{2+} and Fe^{3+} sites within MOF-235(Fe) enables it to function as a solid-state analog of Fenton reagents in advanced oxidation processes (AOPs), facilitating the degradation of MB in solution through H_2O_2-derived reactive species.[229]

Beyond dye adsorption, MOFs have also been developed as highly efficient platforms for heavy metal ion removal. Zhong and co-workers reported a versatile MOF-based broad-spectrum

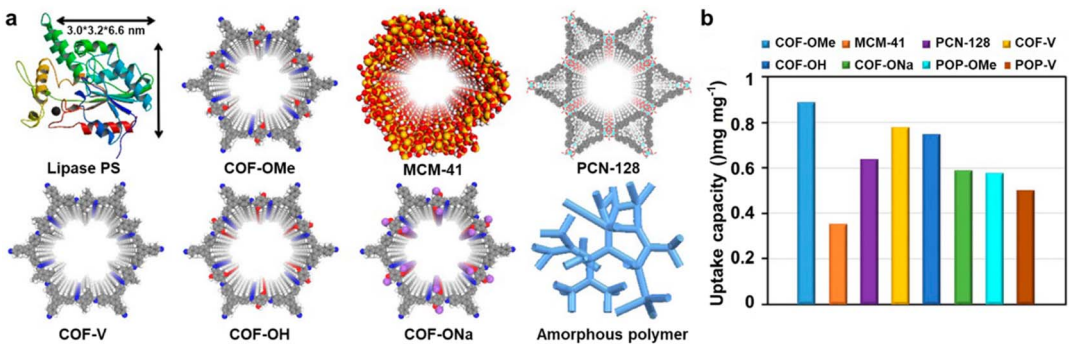

Fig. 14 (a) Schematic representation of lipase PS and porous materials used for enzyme immobilization (blue: N, gray: C, red: O, white: H, yellow: Si, purple: Na). (b) Enzyme uptake capacity of various porous materials after 6 hours of incubation in a 30 mg per mL lipase PS solution. Reproduced with permission.[225] Copyright 2018, American Chemical Society.

heavy metal ion trap, capable of capturing a total of 22 different heavy metal ions, encompassing hard, soft, and borderline Lewis metal ions (Fig. 15).[230] This MOF material, derived from MOF-808(Zr) (constructed from BTC and $ZrOCl_2 \cdot 8H_2O$),[231,232] was post-synthetically modified through a solvent-assisted linker exchange method, where the formate groups on the Zr_6 clusters were replaced with EDTA, yielding MOF-808-EDTA (BS-HMT). This modification introduced highly efficient chelating sites within the MOF's pores, significantly enhancing its heavy metal binding capabilities. The modified MOF demonstrated ultrahigh removal efficiencies (>99%) for all 22 tested metal ions, irrespective of their classification as soft, hard, or borderline acids. The exceptional performance of BS-HMT highlights how pore chemistry in MOFs can be effectively tuned through simple PSM strategies, broadening their application in selective pollutant separation and environmental remediation. This research underscores the vast potential of MOFs and COFs as tunable, high-performance materials for environmental applications, offering sustainable and efficient solutions for pollutant removal and resource recovery.

Our group developed a series of post-synthetically modified COFs functionalized with various thiol groups and demonstrated their efficacy in mercury removal. We designed a vinyl-functionalized monomer, 2,5-divinylterephthalaldehyde, in which the vinyl groups remain intact during COF synthesis, allowing for further chemical modifications.[233] The resulting vinyl-functionalized COF (COF-V) was synthesized *via* the condensation of 2,5-divinylterephthalaldehyde and TPB. Given the strong affinity of sulfur-containing groups for soft heavy metal species like mercury and the high efficiency of thiol-ene click chemistry, a library of thiol compounds with varying flexibility and sulfur densities was selected to react with the vinyl groups on the COF pore surface. The modified sulfur-functionalized COFs retained their crystallinity and porosity, enabling effective mercury removal from both aqueous solutions and the gas phase. These COFs exhibited outstanding uptake capacities of up to 1350 mg g^{-1} (at an equilibrium concentration of 110 ppm) for Hg^{2+} and 863 mg g^{-1} for Hg^0. Additionally, they could rapidly reduce Hg^{2+} concentrations to as low as 0.1 ppb, even in the presence of high concentrations of competing ions. Notably, the flexibility of the chelating groups influenced mercury accessibility, demonstrating that the capture and adsorption performance of COF-based adsorbents can be precisely tailored through pore engineering.

Building on the versatile chemical modification potential of COF-V, we further integrated superwettability into COFs by treating COF-V with 1*H*,1*H*,2*H*,2*H*-perfluorodecanethiol *via* thiol-ene click chemistry to yield COF-VF (Fig. 16).[234] The successful incorporation of perfluoroalkyl groups onto the COF pore surface was confirmed by water contact angle (CA) measurements. COF-VF exhibited a static water CA of approximately 167°, indicating a superhydrophobic surface, whereas COF-V and its alkyl-modified derivative showed CAs of only 113° and 122°, respectively. In contrast, oil droplets were instantly absorbed upon contact with COF-VF, confirming its superhydrophobic and superoleophilic properties. To explore its practical applications, COF-VF was integrated into commercial melamine foams, resulting in a cost-effective superhydrophobic foam (COF-VF@foam). This was achieved by immersing monolithic melamine foam in a precursor solution, followed by solvothermal synthesis to *in situ* coat COF-V onto the foam structure. Subsequent grafting of perfluoroalkyl groups onto the COF-V coating produced COF-VF@foam. The uptake performance of COF-VF@foam was evaluated using various organic liquids, demonstrating sorption capacities ranging from 67 to 142 times its own weight, highlighting its potential for oil-spill cleanup. Furthermore, COF-VF@foam exhibited excellent recyclability. The foam-based adsorbent could be easily regenerated by squeezing out the absorbed oil, maintaining its performance over at least ten adsorption cycles without significant efficiency loss. These results demonstrate that superhydrophobicity can be effectively incorporated into COFs through pore-surface

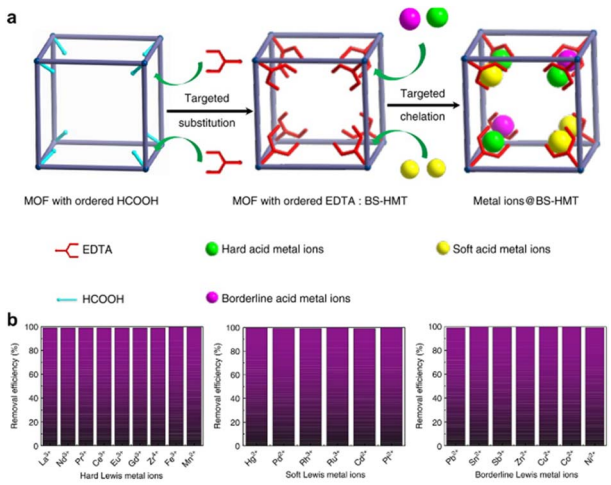

Fig. 15 (a) Schematic illustration of the BS-HMT concept. Ordered HCOOH molecules in MOF-808 can be replaced by EDTA, leading to MOF-808 with an ordered EDTA arrangement, which functions as a BS-HMT for metal ion capture. (b) The removal efficiency of hard Lewis metal ions, soft Lewis metal ions, and borderline Lewis metal ions for MOF-808-EDTA. Reproduced with permission.[230] Copyright 2018, Springer Nature.

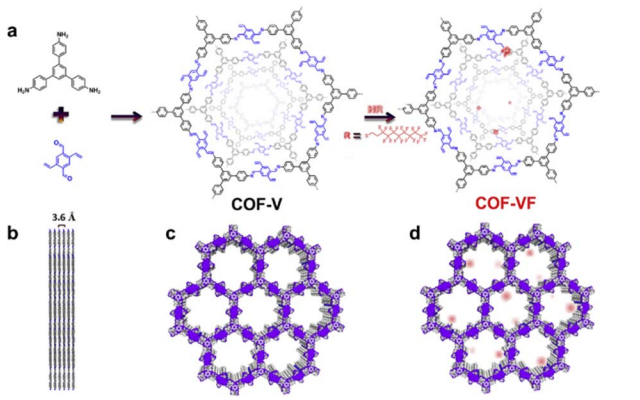

Fig. 16 Schematic illustration of imparting superhydrophobicity on COF-V. (a) Synthetic scheme of COF-V and COF-VF. (b and c) Schematic representation of the eclipsed AA stacking structure of COF-V. (d) Schematic representation of COF-VF. Reproduced with permission.[234] Copyright 2018, Elsevier.

engineering, offering valuable insights into structure–property relationships between functional groups and practical applications.

MOFs and COFs have demonstrated superior radionuclide sequestration performance compared to traditional porous materials, offering enhanced uptake capacity and selectivity. Carboni *et al.* pioneered the application of MOFs as novel sorbents for actinide extraction from aqueous media.[235] Specifically, they synthesized three MOFs with UiO-68 network topology using amino-TPDC or TPDC bridging ligands functionalized with orthogonal phosphorylurea groups (TPDC = *p*,*p*′-terphenyldicarboxylic acid). Among them, the UiO-MOF with diethoxyphosphorylurea functionalization [UiO-68-P(O)$(OEt)_2$, MOF 2] was synthesized from $ZrCl_4$ and a diethoxyphosphorylurea-derived TPDC ligand (H_2L_2), obtained through the condensation of 2′-amino-1,1′:4′,1″-terphenyl-4,4″-dicarboxylic acid (H_2tpdc-NH_2) with diethoxyphosphinyl isocyanate. MOF 2 exhibited near-quantitative uranium removal from both water and artificial seawater, achieving a remarkable saturation sorption capacity of 217 mg U per g, corresponding to the binding of one uranyl ion per two phosphorylurea groups. Building upon this progress, our group designed and synthesized a novel, highly stable carboxylated MOF, BUT-12-3COOH, featuring an ultra-high density of free carboxyl groups, exceptional chemical stability, rapid adsorption kinetics, and a high U(VI) sorption capacity.[236] Through precise pore engineering, we optimized the pore environment of BUT-12-3COOH to maximize uranium capture efficiency, achieving an impressive maximum sorption capacity of 235 mg U per g, demonstrating its outstanding extraction ability from aqueous solutions.

Beyond MOFs, our group proposed a pore-environment engineering strategy to optimize COFs for radionuclide sequestration.[237–240] Given that amidoxime is the state-of-the-art functional moiety for uranium capture, we incorporated amidoxime groups into COFs *via* a two-step synthesis (Fig. 17).[241] First, a nitrile-functionalized COF (COF-TpDb) was synthesized by condensing 2,5-diaminobenzonitrile (Db) with Tp under solvothermal conditions, aligning cyano groups within the 1D pore channels. These cyano groups were subsequently converted into amidoxime moieties through hydroxylamine treatment, yielding an amidoxime-functionalized COF adsorbent (COF-TpDb-AO). Through this pore-surface functionalization approach, the eclipsed stacking arrangement of 2D extended polygons in COF-TpDb-AO positions the amidoxime chelating groups in adjacent layers parallel to each other, facilitating cooperative interactions for enhanced uranium binding. As a result, COF-TpDb-AO exhibited far superior adsorption performance compared to its amorphous analog (POP-TpDb-AO), with saturation adsorption capacities of 408 mg U per g and 355 mg U per g, respectively. Notably, COF-TpDb-AO reduced uranium concentrations in contaminated water samples from 1 ppm to below 0.1 ppb within minutes, surpassing the stringent drinking water limit (30 ppb). Moreover, in spiked seawater, it achieved an exceptionally high uranium uptake of 127 mg U per g, illustrating its potential for uranium mining applications. These findings highlight the critical role of pore engineering in MOFs and COFs,

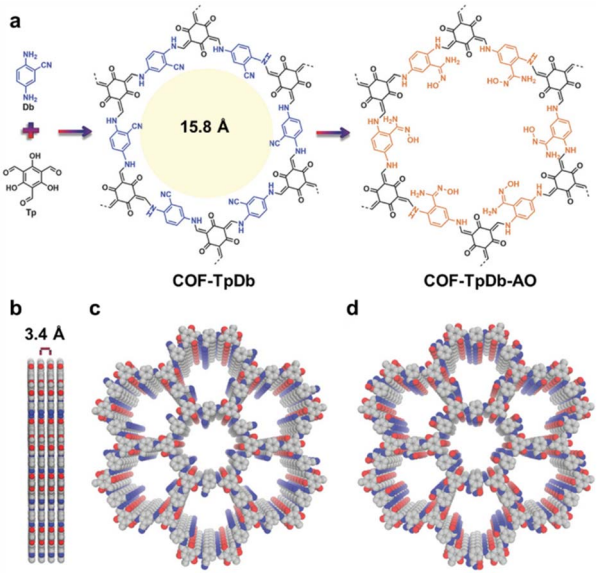

Fig. 17 (a) Synthetic scheme of COF-TpDb, formed through the condensation of Tp (black) and Db (blue), followed by a chemical transformation of cyano groups into amidoxime groups, yielding COF-TpDb-AO. (b and c) Schematic representation of the eclipsed AA stacking structure of COF-TpDb (blue: N; gray: C; red: O; hydrogen omitted for clarity). (d) Schematic representation of COF-TpDb-AO (blue: N; gray: C; red: O; hydrogen omitted for clarity). Reproduced with permission.[241] Copyright 2018, John Wiley and Sons.

demonstrating how precise functionalization and tailored pore environments can significantly enhance their performance in environmental remediation, particularly for radionuclide sequestration.

4. Outlooks and conclusion

In this review, we provide a comprehensive and timely overview of the advancements in pore engineering of MOFs and COFs, highlighting how precise modifications in pore structures and surface chemistry can significantly enhance their functionality and expand their applicability across various domains. We discuss in detail the strategies employed to functionalize and tailor these crystalline porous frameworks, including *de novo* synthesis and post-synthetic modifications. Furthermore, drawing from our extensive research experience in gas storage and separation, catalysis, and environmental remediation, we discuss the design principles and strategic approaches for optimizing MOFs and COFs in these applications. We highlight how rational pore engineering, through precise control over pore size, topology, and surface chemistry, enhances adsorption capacity, selectivity, and stability. Building on our group's advancements, we illustrate how these pore-engineered frameworks surpass conventional porous materials by exhibiting superior efficiency, accelerated kinetics, and enhanced recyclability, thereby broadening their practical applicability. Through precise control over composition, pore geometry, and surface functionality, MOFs and COFs can be strategically tailored for specific applications, paving the way for next-generation materials with optimized performance and

expanded functionality. This review not only provides insight into the current state-of-the-art in pore engineering but also sheds light on future research directions and challenges that need to be addressed for broader industrial implementation.

Despite significant advancements, the practical application of MOFs and COFs remains challenging, particularly in scalable synthesis and processing.[242–245] High production costs and low yields often hinder large-scale manufacturing. Addressing these issues requires the development of cost-effective organic ligands and monomers alongside more efficient, sustainable synthesis strategies that improve yield while reducing energy consumption and waste. In addition to synthetic challenges, the chemical and mechanical stability, as well as the recyclability of MOFs and COFs under harsh industrial conditions—such as exposure to moisture, high temperature, or chemical contaminants—pose significant barriers to their long-term deployment. Many MOFs and COFs exhibit degradation or loss of structural integrity upon repeated use, which limits their feasibility in continuous operation environments such as adsorption-based separation or catalytic cycles. Therefore, improving the robustness and reusability of these materials is essential for real-world applications. Additionally, the complex and often multistep synthesis required for designing task-specific MOFs and COFs presents another hurdle to their large-scale adoption. To address this, future research should prioritize the development of more streamlined and scalable synthetic strategies that retain key structural features such as crystallinity, porosity, and stability. Furthermore, progress in material processing—such as shaping MOFs and COFs into membranes,[246,247] monoliths,[248–250] or composites structures[251–254]—will be vital to bridge the gap between laboratory research and practical applications.

Artificial intelligence (AI) and machine learning (ML) offer transformative solutions by enabling data-driven crystalline porous material design.[255–262] ML algorithms can analyze vast chemical datasets, predict structure–property relationships, and optimize synthetic pathways, significantly reducing reliance on trial-and-error experimentation. AI-driven models facilitate high-throughput screening of candidate frameworks, accelerating the discovery of MOFs and COFs with tailored adsorption, separation, and catalytic properties. Deep learning further refines this process by predicting material stability, porosity, and functional performance before synthesis, streamlining development. In pore engineering, AI enables precise modulation of pore environments to enhance material selectivity and efficiency. Advanced ML models uncover correlations between pore structure and host–guest interactions, guiding the rational design of highly selective materials. Generative algorithms, including deep neural networks and reinforcement learning, can autonomously propose novel MOF and COF architectures with optimized pore chemistry and spatial configurations. AI-driven robotic synthesis platforms further enhance reproducibility and accelerate the experimental validation of computationally designed structures, bridging the gap between theoretical predictions and practical applications.

In the future, integrating AI with MOF and COF research will revolutionize material innovation, making it more predictive, scalable, and application-driven. By merging AI-guided discovery with advanced synthesis techniques, next-generation crystalline porous materials can be precisely engineered, unlocking breakthroughs in a variety of practical applications.

Data availability

The data that support the findings of this study are available from the corresponding author, S. Ma, upon reasonable request.

Author contributions

Yanpei Song: conceptualization, methodology, writing – original draft, visualization; Shengqian Ma: investigation, funding acquisition, writing – review & editing, validation, supervision.

Conflicts of interest

There are no conflicts to declare.

Acknowledgements

The authors acknowledge the financial support from the Robert A. Welch Foundation (B-0027) for this work.

References

1 Y. Li, L. Li and J. Yu, Applications of Zeolites in Sustainable Chemistry, *Chem*, 2017, **3**, 928–949.
2 X. Meng and F. S. Xiao, Green routes for synthesis of zeolites, *Chem. Rev.*, 2014, **114**, 1521–1543.
3 M. Dusselier and M. E. Davis, Small-Pore Zeolites: Synthesis and Catalysis, *Chem. Rev.*, 2018, **118**, 5265–5329.
4 H. Furukawa, K. E. Cordova, M. O'Keeffe and O. M. Yaghi, The chemistry and applications of metal-organic frameworks, *Science*, 2013, **341**, 1230444.
5 H. C. Zhou, J. R. Long and O. M. Yaghi, Introduction to metal-organic frameworks, *Chem. Rev.*, 2012, **112**, 673–674.
6 N. Stock and S. Biswas, Synthesis of metal-organic frameworks (MOFs): routes to various MOF topologies, morphologies, and composites, *Chem. Rev.*, 2012, **112**, 933–969.
7 A. J. Howarth, Y. Liu, P. Li, Z. Li, T. C. Wang, J. T. Hupp and O. K. Farha, Chemical, thermal and mechanical stabilities of metal–organic frameworks, *Nat. Rev. Mater.*, 2016, **1**, 15018.
8 H. C. Zhou and S. Kitagawa, Metal-organic frameworks (MOFs), *Chem. Soc. Rev.*, 2014, **43**, 5415–5418.
9 M. Ding, X. Cai and H. L. Jiang, Improving MOF stability: approaches and applications, *Chem. Sci.*, 2019, **10**, 10209–10230.
10 Y. Song, Q. Sun, B. Aguila and S. Ma, Opportunities of Covalent Organic Frameworks for Advanced Applications, *Adv. Sci.*, 2019, **6**, 1801410.
11 C. S. Diercks and O. M. Yaghi, The atom, the molecule, and the covalent organic framework, *Science*, 2017, **355**, aal1585.

12 S. Kandambeth, K. Dey and R. Banerjee, Covalent Organic Frameworks: Chemistry beyond the Structure, *J. Am. Chem. Soc.*, 2019, **141**, 1807–1822.
13 K. Geng, T. He, R. Liu, S. Dalapati, K. T. Tan, Z. Li, S. Tao, Y. Gong, Q. Jiang and D. Jiang, Covalent Organic Frameworks: Design, Synthesis, and Functions, *Chem. Rev.*, 2020, **120**, 8814–8933.
14 S. Y. Ding and W. Wang, Covalent organic frameworks (COFs): from design to applications, *Chem. Soc. Rev.*, 2013, **42**, 548–568.
15 X. Feng, X. Ding and D. Jiang, Covalent organic frameworks, *Chem. Soc. Rev.*, 2012, **41**, 6010–6022.
16 R.-B. Lin and B. Chen, Hydrogen-bonded organic frameworks: Chemistry and functions, *Chem*, 2022, **8**, 2114–2135.
17 R. B. Lin, Y. He, P. Li, H. Wang, W. Zhou and B. Chen, Multifunctional porous hydrogen-bonded organic framework materials, *Chem. Soc. Rev.*, 2019, **48**, 1362–1389.
18 B. Wang, R. B. Lin, Z. Zhang, S. Xiang and B. Chen, Hydrogen-Bonded Organic Frameworks as a Tunable Platform for Functional Materials, *J. Am. Chem. Soc.*, 2020, **142**, 14399–14416.
19 D. Yu, H. Zhang, J. Ren and X. Qu, Hydrogen-bonded organic frameworks: new horizons in biomedical applications, *Chem. Soc. Rev.*, 2023, **52**, 7504–7523.
20 Z. Zhang, Y. Ye, S. Xiang and B. Chen, Exploring Multifunctional Hydrogen-Bonded Organic Framework Materials, *Acc. Chem. Res.*, 2022, **55**, 3752–3766.
21 R. Freund, O. Zaremba, G. Arnauts, R. Ameloot, G. Skorupskii, M. Dinca, A. Bavykina, J. Gascon, A. Ejsmont, J. Goscianska, M. Kalmutzki, U. Lachelt, E. Ploetz, C. S. Diercks and S. Wuttke, The Current Status of MOF and COF Applications, *Angew. Chem., Int. Ed.*, 2021, **60**, 23975–24001.
22 E. Ploetz, H. Engelke, U. Lächelt and S. Wuttke, The Chemistry of Reticular Framework Nanoparticles: MOF, ZIF, and COF Materials, *Adv. Funct. Mater.*, 2020, **30**, 1909062.
23 Y. Li, M. Karimi, Y.-N. Gong, N. Dai, V. Safarifard and H.-L. Jiang, Integration of metal-organic frameworks and covalent organic frameworks: Design, synthesis, and applications, *Matter*, 2021, **4**, 2230–2265.
24 Z. Heidarinejad, M. H. Dehghani, M. Heidari, G. Javedan, I. Ali and M. Sillanpää, Methods for preparation and activation of activated carbon: a review, *Environ. Chem. Lett.*, 2020, **18**, 393–415.
25 C. Martínez and A. Corma, Inorganic molecular sieves: Preparation, modification and industrial application in catalytic processes, *Coord. Chem. Rev.*, 2011, **255**, 1558–1580.
26 S.-H. Wu, C.-Y. Mou and H.-P. Lin, Synthesis of mesoporous silica nanoparticles, *Chem. Soc. Rev.*, 2013, **42**, 3862–3875.
27 R.-J. Wei, X. Luo and D. Li, Covalent Metal–Organic Frameworks: Fusion of Covalent Organic Frameworks and Metal–Organic Frameworks, *Acc. Chem. Res.*, 2025, **58**, 746–761.
28 I. M. Honicke, I. Senkovska, V. Bon, I. A. Baburin, N. Bonisch, S. Raschke, J. D. Evans and S. Kaskel, Balancing Mechanical Stability and Ultrahigh Porosity in Crystalline Framework Materials, *Angew. Chem., Int. Ed.*, 2018, **57**, 13780–13783.
29 L. A. Baldwin, J. W. Crowe, D. A. Pyles and P. L. McGrier, Metalation of a Mesoporous Three-Dimensional Covalent Organic Framework, *J. Am. Chem. Soc.*, 2016, **138**, 15134–15137.
30 W. Fan, X. Zhang, Z. Kang, X. Liu and D. Sun, Isoreticular chemistry within metal–organic frameworks for gas storage and separation, *Coord. Chem. Rev.*, 2021, **443**, 213968.
31 X. Zhao, Y. Wang, D. S. Li, X. Bu and P. Feng, Metal-Organic Frameworks for Separation, *Adv. Mater.*, 2018, **30**, e1705189.
32 J. R. Li, R. J. Kuppler and H. C. Zhou, Selective gas adsorption and separation in metal-organic frameworks, *Chem. Soc. Rev.*, 2009, **38**, 1477–1504.
33 Q. Yang, D. Liu, C. Zhong and J. R. Li, Development of computational methodologies for metal-organic frameworks and their application in gas separations, *Chem. Rev.*, 2013, **113**, 8261–8323.
34 A. Knebel and J. Caro, Metal-organic frameworks and covalent organic frameworks as disruptive membrane materials for energy-efficient gas separation, *Nat. Nanotechnol.*, 2022, **17**, 911–923.
35 Z. Wang, S. Zhang, Y. Chen, Z. Zhang and S. Ma, Covalent organic frameworks for separation applications, *Chem. Soc. Rev.*, 2020, **49**, 708–735.
36 B. Hosseini Monjezi, K. Kutonova, M. Tsotsalas, S. Henke and A. Knebel, Current Trends in Metal-Organic and Covalent Organic Framework Membrane Materials, *Angew. Chem., Int. Ed.*, 2021, **60**, 15153–15164.
37 S. Yuan, X. Li, J. Zhu, G. Zhang, P. Van Puyvelde and B. Van der Bruggen, Covalent organic frameworks for membrane separation, *Chem. Soc. Rev.*, 2019, **48**, 2665–2681.
38 S. M. J. Rogge, A. Bavykina, J. Hajek, H. Garcia, A. I. Olivos-Suarez, A. Sepulveda-Escribano, A. Vimont, G. Clet, P. Bazin, F. Kapteijn, M. Daturi, E. V. Ramos-Fernandez, I. X. F. X. Llabres, V. Van Speybroeck and J. Gascon, Metal-organic and covalent organic frameworks as single-site catalysts, *Chem. Soc. Rev.*, 2017, **46**, 3134–3184.
39 A. Dhakshinamoorthy, Z. Li and H. Garcia, Catalysis and photocatalysis by metal organic frameworks, *Chem. Soc. Rev.*, 2018, **47**, 8134–8172.
40 Y. B. Huang, J. Liang, X. S. Wang and R. Cao, Multifunctional metal-organic framework catalysts: synergistic catalysis and tandem reactions, *Chem. Soc. Rev.*, 2017, **46**, 126–157.
41 L. Zhu, X. Q. Liu, H. L. Jiang and L. B. Sun, Metal-Organic Frameworks for Heterogeneous Basic Catalysis, *Chem. Rev.*, 2017, **117**, 8129–8176.
42 W. Zhao, Q. Zhu, X. Wu and D. Zhao, The development of catalysts and auxiliaries for the synthesis of covalent organic frameworks, *Chem. Soc. Rev.*, 2024, **53**, 7531–7565.

43 A. Bavykina, N. Kolobov, I. S. Khan, J. A. Bau, A. Ramirez and J. Gascon, Metal-Organic Frameworks in Heterogeneous Catalysis: Recent Progress, New Trends, and Future Perspectives, *Chem. Rev.*, 2020, **120**, 8468–8535.
44 D. Li, H.-Q. Xu, L. Jiao and H.-L. Jiang, Metal-organic frameworks for catalysis: State of the art, challenges, and opportunities, *EnergyChem*, 2019, **1**, 100005.
45 X. Meng, H. N. Wang, S. Y. Song and H. J. Zhang, Proton-conducting crystalline porous materials, *Chem. Soc. Rev.*, 2017, **46**, 464–480.
46 D. W. Lim and H. Kitagawa, Rational strategies for proton-conductive metal-organic frameworks, *Chem. Soc. Rev.*, 2021, **50**, 6349–6368.
47 Y. Ye, L. Gong, S. Xiang, Z. Zhang and B. Chen, Metal-Organic Frameworks as a Versatile Platform for Proton Conductors, *Adv. Mater.*, 2020, **32**, e1907090.
48 D. W. Lim and H. Kitagawa, Proton Transport in Metal-Organic Frameworks, *Chem. Rev.*, 2020, **120**, 8416–8467.
49 R. Sahoo, S. Mondal, S. C. Pal, D. Mukherjee and M. C. Das, Covalent-Organic Frameworks (COFs) as Proton Conductors, *Adv. Energy Mater.*, 2021, **11**, 2102300.
50 H. Xu, S. Tao and D. Jiang, Proton conduction in crystalline and porous covalent organic frameworks, *Nat. Mater.*, 2016, **15**, 722–726.
51 L. E. Kreno, K. Leong, O. K. Farha, M. Allendorf, R. P. Van Duyne and J. T. Hupp, Metal-organic framework materials as chemical sensors, *Chem. Rev.*, 2012, **112**, 1105–1125.
52 Z. Meng and K. A. Mirica, Covalent organic frameworks as multifunctional materials for chemical detection, *Chem. Soc. Rev.*, 2021, **50**, 13498–13558.
53 Z. Hu, B. J. Deibert and J. Li, Luminescent metal-organic frameworks for chemical sensing and explosive detection, *Chem. Soc. Rev.*, 2014, **43**, 5815–5840.
54 X. Liu, D. Huang, C. Lai, G. Zeng, L. Qin, H. Wang, H. Yi, B. Li, S. Liu, M. Zhang, R. Deng, Y. Fu, L. Li, W. Xue and S. Chen, Recent advances in covalent organic frameworks (COFs) as a smart sensing material, *Chem. Soc. Rev.*, 2019, **48**, 5266–5302.
55 L. Guo, L. Yang, M. Li, L. Kuang, Y. Song and L. Wang, Covalent organic frameworks for fluorescent sensing: Recent developments and future challenges, *Coord. Chem. Rev.*, 2021, **440**, 213957.
56 W.-T. Koo, J.-S. Jang and I.-D. Kim, Metal-Organic Frameworks for Chemiresistive Sensors, *Chem*, 2019, **5**, 1938–1963.
57 I. Ahmed and S. H. Jhung, Covalent organic framework-based materials: Synthesis, modification, and application in environmental remediation, *Coord. Chem. Rev.*, 2021, **441**, 213989.
58 S. Daliran, A. R. Oveisi, C. W. Kung, U. Sen, A. Dhakshinamoorthy, C. H. Chuang, M. Khajeh, M. Erkartal and J. T. Hupp, Defect-enabling zirconium-based metal-organic frameworks for energy and environmental remediation applications, *Chem. Soc. Rev.*, 2024, **53**, 6244–6294.
59 S. Ge, K. Wei, W. Peng, R. Huang, E. Akinlabi, H. Xia, M. W. Shahzad, X. Zhang, B. B. Xu and J. Jiang, A comprehensive review of covalent organic frameworks (COFs) and their derivatives in environmental pollution control, *Chem. Soc. Rev.*, 2024, **53**, 11259–11302.
60 J. Wang and S. Zhuang, Covalent organic frameworks (COFs) for environmental applications, *Coord. Chem. Rev.*, 2019, **400**, 213046.
61 S. Dhaka, R. Kumar, A. Deep, M. B. Kurade, S.-W. Ji and B.-H. Jeon, Metal–organic frameworks (MOFs) for the removal of emerging contaminants from aquatic environments, *Coord. Chem. Rev.*, 2019, **380**, 330–352.
62 S. Rojas and P. Horcajada, Metal-Organic Frameworks for the Removal of Emerging Organic Contaminants in Water, *Chem. Rev.*, 2020, **120**, 8378–8415.
63 O. K. Farha and J. T. Hupp, *Acc. Chem. Res.*, 2010, **43**, 1166–1175.
64 F. A. Paz, J. Klinowski, S. M. Vilela, J. P. Tome, J. A. Cavaleiro and J. Rocha, Ligand design for functional metal-organic frameworks, *Chem. Soc. Rev.*, 2012, **41**, 1088–1110.
65 W. Lu, Z. Wei, Z.-Y. Gu, T.-F. Liu, J. Park, J. Park, J. Tian, M. Zhang, Q. Zhang and T. Gentle Iii, Tuning the structure and function of metal–organic frameworks *via* linker design, *Chem. Soc. Rev.*, 2014, **43**, 5561–5593.
66 K. Wang, K. N. Hui, K. San Hui, S. Peng and Y. Xu, Recent progress in metal-organic framework/graphene-derived materials for energy storage and conversion: design, preparation, and application, *Chem. Sci.*, 2021, **12**, 5737–5766.
67 X. Guan, F. Chen, Q. Fang and S. Qiu, Design and applications of three dimensional covalent organic frameworks, *Chem. Soc. Rev.*, 2020, **49**, 1357–1384.
68 B. Gui, G. Lin, H. Ding, C. Gao, A. Mal and C. Wang, Three-Dimensional Covalent Organic Frameworks: From Topology Design to Applications, *Acc. Chem. Res.*, 2020, **53**, 2225–2234.
69 X. Han, C. Yuan, B. Hou, L. Liu, H. Li, Y. Liu and Y. Cui, Chiral covalent organic frameworks: design, synthesis and property, *Chem. Soc. Rev.*, 2020, **49**, 6248–6272.
70 H. Li, M. Eddaoudi, M. O'Keeffe and O. M. Yaghi, Design and synthesis of an exceptionally stable and highly porous metal-organic framework, *Nature*, 1999, **402**, 276–279.
71 H. Li, M. Eddaoudi, T. L. Groy and O. M. Yaghi, Establishing microporosity in open metal–organic frameworks: gas sorption isotherms for Zn (BDC)(BDC= 1, 4-benzenedicarboxylate), *J. Am. Chem. Soc.*, 1998, **120**, 8571–8572.
72 M. Y. Masoomi, A. Morsali, A. Dhakshinamoorthy and H. Garcia, Mixed-Metal MOFs: Unique Opportunities in Metal-Organic Framework (MOF) Functionality and Design, *Angew. Chem., Int. Ed.*, 2019, **58**, 15188–15205.
73 L. J. Wang, H. Deng, H. Furukawa, F. Gandara, K. E. Cordova, D. Peri and O. M. Yaghi, Synthesis and characterization of metal-organic framework-74 containing 2, 4, 6, 8, and 10 different metals, *Inorg. Chem.*, 2014, **53**, 5881–5883.
74 H. Deng, C. Doonan, H. Furukawa, R. Ferreira, J. Towne, C. Knobler, B. Wang and O. Yaghi, Multiple functional

groups of varying ratios in metal-organic frameworks, *Science*, 2010, **327**, 846–850.

75 M. Wang, T. Zeng, Y. Yu, X. Wang, Y. Zhao, H. Xi and Y. B. Zhang, Flexibility On-Demand: Multivariate 3D Covalent Organic Frameworks, *J. Am. Chem. Soc.*, 2024, **146**, 1035–1041.

76 S. K. Sobczak, J. Drweska, W. Gromelska, K. Roztocki and A. M. Janiak, Multivariate Flexible Metal-Organic Frameworks and Covalent Organic Frameworks, *Small*, 2024, **20**, e2402486.

77 X. Yin, A. Alsuwaidi and X. Zhang, Hierarchical metal-organic framework (MOF) pore engineering, *Microporous Mesoporous Mater.*, 2022, **330**, 111633.

78 A. P. Cote, A. I. Benin, N. W. Ockwig, M. O'Keeffe, A. J. Matzger and O. M. Yaghi, Porous, crystalline, covalent organic frameworks, *Science*, 2005, **310**, 1166–1170.

79 J. L. Segura, M. J. Mancheno and F. Zamora, Covalent organic frameworks based on Schiff-base chemistry: synthesis, properties and potential applications, *Chem. Soc. Rev.*, 2016, **45**, 5635–5671.

80 F. J. Uribe-Romo, J. R. Hunt, H. Furukawa, C. Klöck, M. O'Keeffe and O. M. Yaghi, A crystalline imine-linked 3-D porous covalent organic framework, *J. Am. Chem. Soc.*, 2009, **131**, 4570–4571.

81 L. Stegbauer, K. Schwinghammer and B. V. Lotsch, A hydrazone-based covalent organic framework for photocatalytic hydrogen production, *Chem. Sci.*, 2014, **5**, 2789–2793.

82 F. J. Uribe-Romo, C. J. Doonan, H. Furukawa, K. Oisaki and O. M. Yaghi, Crystalline covalent organic frameworks with hydrazone linkages, *J. Am. Chem. Soc.*, 2011, **133**, 11478–11481.

83 S. Dalapati, S. Jin, J. Gao, Y. Xu, A. Nagai and D. Jiang, An azine-linked covalent organic framework, *J. Am. Chem. Soc.*, 2013, **135**, 17310–17313.

84 V. S. Vyas, F. Haase, L. Stegbauer, G. Savasci, F. Podjaski, C. Ochsenfeld and B. V. Lotsch, A tunable azine covalent organic framework platform for visible light-induced hydrogen generation, *Nat. Commun.*, 2015, **6**, 8508.

85 W. Zhou, Q. W. Deng, H. J. He, L. Yang, T. Y. Liu, X. Wang, D. Y. Zheng, Z. B. Dai, L. Sun, C. Liu, H. Wu, Z. Li and W. Q. Deng, Heterogenization of Salen Metal Molecular Catalysts in Covalent Organic Frameworks for Photocatalytic Hydrogen Evolution, *Angew. Chem., Int. Ed.*, 2023, **62**, e202214143.

86 H. Li, X. Feng, P. Shao, J. Chen, C. Li, S. Jayakumar and Q. Yang, Synthesis of covalent organic frameworks *via in situ* salen skeleton formation for catalytic applications, *J. Mater. Chem. A*, 2019, **7**, 5482–5492.

87 S. Kandambeth, A. Mallick, B. Lukose, M. V. Mane, T. Heine and R. Banerjee, Construction of crystalline 2D covalent organic frameworks with remarkable chemical (acid/base) stability *via* a combined reversible and irreversible route, *J. Am. Chem. Soc.*, 2012, **134**, 19524–19527.

88 C. R. DeBlase, K. E. Silberstein, T. T. Truong, H. D. Abruna and W. R. Dichtel, beta-Ketoenamine-linked covalent organic frameworks capable of pseudocapacitive energy storage, *J. Am. Chem. Soc.*, 2013, **135**, 16821–16824.

89 M. A. Khayum, M. Ghosh, V. Vijayakumar, A. Halder, M. Nurhuda, S. Kumar, M. Addicoat, S. Kurungot and R. Banerjee, Zinc ion interactions in a two-dimensional covalent organic framework based aqueous zinc ion battery, *Chem. Sci.*, 2019, **10**, 8889–8894.

90 Q. Fang, J. Wang, S. Gu, R. B. Kaspar, Z. Zhuang, J. Zheng, H. Guo, S. Qiu and Y. Yan, 3D Porous Crystalline Polyimide Covalent Organic Frameworks for Drug Delivery, *J. Am. Chem. Soc.*, 2015, **137**, 8352–8355.

91 Q. Fang, Z. Zhuang, S. Gu, R. B. Kaspar, J. Zheng, J. Wang, S. Qiu and Y. Yan, Designed synthesis of large-pore crystalline polyimide covalent organic frameworks, *Nat. Commun.*, 2014, **5**, 4503.

92 X. Chen, Q. Dang, R. Sa, L. Li, L. Li, J. Bi, Z. Zhang, J. Long, Y. Yu and Z. Zou, Integrating single Ni sites into biomimetic networks of covalent organic frameworks for selective photoreduction of CO_2, *Chem. Sci.*, 2020, **11**, 6915–6922.

93 T. X. Luan, L. Du, J. R. Wang, K. Li, Q. Zhang, P. Z. Li and Y. Zhao, Highly Effective Generation of Singlet Oxygen by an Imidazole-Linked Robust Photosensitizing Covalent Organic Framework, *ACS Nano*, 2022, **16**, 21565–21575.

94 Y. Zhang, Z. Qiao, R. Zhang, Z. Wang, H. J. Wang, J. Zhao, D. Cao and S. Wang, Multicomponent Synthesis of Imidazole-Linked Fully Conjugated 3D Covalent Organic Framework for Efficient Electrochemical Hydrogen Peroxide Production, *Angew. Chem., Int. Ed.*, 2023, **62**, e202314539.

95 M. D. Zhang, J. R. Huang, W. Shi, P. Q. Liao and X. M. Chen, Self-Accelerating Effect in a Covalent-Organic Framework with Imidazole Groups Boosts Electroreduction of CO_2 to CO, *Angew. Chem., Int. Ed.*, 2023, **62**, e202308195.

96 P. F. Wei, M. Z. Qi, Z. P. Wang, S. Y. Ding, W. Yu, Q. Liu, L. K. Wang, H. Z. Wang, W. K. An and W. Wang, Benzoxazole-Linked Ultrastable Covalent Organic Frameworks for Photocatalysis, *J. Am. Chem. Soc.*, 2018, **140**, 4623–4631.

97 C. J. Wu, X. Y. Li, T. R. Li, M. Z. Shao, L. J. Niu, X. F. Lu, J. L. Kan, Y. Geng and Y. B. Dong, Natural Sunlight Photocatalytic Synthesis of Benzoxazole-Bridged Covalent Organic Framework for Photocatalysis, *J. Am. Chem. Soc.*, 2022, **144**, 18750–18755.

98 D. A. Pyles, W. H. Coldren, G. M. Eder, C. M. Hadad and P. L. McGrier, Mechanistic investigations into the cyclization and crystallization of benzobisoxazole-linked two-dimensional covalent organic frameworks, *Chem. Sci.*, 2018, **9**, 6417–6423.

99 C. Qian, L. Feng, W. L. Teo, J. Liu, W. Zhou, D. Wang and Y. Zhao, Imine and imine-derived linkages in two-dimensional covalent organic frameworks, *Nat. Rev. Chem.*, 2022, **6**, 881–898.

100 S. Xu, M. Richter and X. Feng, Vinylene-Linked Two-Dimensional Covalent Organic Frameworks: Synthesis and Functions, *Acc. Mater. Res.*, 2021, **2**, 252–265.

101 T. He, K. Geng and D. Jiang, All sp^2 carbon covalent organic frameworks, *Trends Chem.*, 2021, **3**, 431–444.

102 Q. Guan, L. L. Zhou and Y. B. Dong, Construction of Covalent Organic Frameworks *via* Multicomponent Reactions, *J. Am. Chem. Soc.*, 2023, **145**, 1475–1496.

103 Z. Meng, A. Aykanat and K. A. Mirica, Proton Conduction in 2D Aza-Fused Covalent Organic Frameworks, *Chem. Mater.*, 2018, **31**, 819–825.

104 J. Feng, Y. J. Zhang, S. H. Ma, C. Yang, Z. P. Wang, S. Y. Ding, Y. Li and W. Wang, Fused-Ring-Linked Covalent Organic Frameworks, *J. Am. Chem. Soc.*, 2022, **144**, 6594–6603.

105 X. Zhuang, W. Zhao, F. Zhang, Y. Cao, F. Liu, S. Bi and X. Feng, A two-dimensional conjugated polymer framework with fully sp^2-bonded carbon skeleton, *Polym. Chem.*, 2016, **7**, 4176–4181.

106 E. Jin, M. Asada, Q. Xu, S. Dalapati, M. A. Addicoat, M. A. Brady, H. Xu, T. Nakamura, T. Heine, Q. Chen and D. Jiang, Two-dimensional sp^2 carbon–conjugated covalent organic frameworks, *Science*, 2017, **357**, 673–676.

107 T. Jadhav, Y. Fang, W. Patterson, C. H. Liu, E. Hamzehpoor and D. F. Perepichka, 2D Poly(arylene vinylene) Covalent Organic Frameworks *via* Aldol Condensation of Trimethyltriazine, *Angew. Chem., Int. Ed.*, 2019, **58**, 13753–13757.

108 D. L. Pastoetter, S. Xu, M. Borrelli, M. Addicoat, B. P. Biswal, S. Paasch, A. Dianat, H. Thomas, R. Berger, S. Reineke, E. Brunner, G. Cuniberti, M. Richter and X. Feng, Synthesis of Vinylene-Linked Two-Dimensional Conjugated Polymers *via* the Horner-Wadsworth-Emmons Reaction, *Angew. Chem., Int. Ed.*, 2020, **59**, 23620–23625.

109 P. Katekomol, J. Roeser, M. Bojdys, J. Weber and A. Thomas, Covalent Triazine Frameworks Prepared from 1,3,5-Tricyanobenzene, *Chem. Mater.*, 2013, **25**, 1542–1548.

110 K. Kamiya, Selective single-atom electrocatalysts: a review with a focus on metal-doped covalent triazine frameworks, *Chem. Sci.*, 2020, **11**, 8339–8349.

111 P. Xiong, S. Zhang, R. Wang, L. Zhang, Q. Ma, X. Ren, Y. Gao, Z. Wang, Z. Guo and C. Zhang, Covalent triazine frameworks for advanced energy storage: challenges and new opportunities, *Energy Environ. Sci.*, 2023, **16**, 3181–3213.

112 M. Liu, L. Guo, S. Jin and B. Tan, Covalent triazine frameworks: synthesis and applications, *J. Mater. Chem. A*, 2019, **7**, 5153–5172.

113 X. Guan, H. Li, Y. Ma, M. Xue, Q. Fang, Y. Yan, V. Valtchev and S. Qiu, Chemically stable polyarylether-based covalent organic frameworks, *Nat. Chem.*, 2019, **11**, 587–594.

114 B. Zhang, M. Wei, H. Mao, X. Pei, S. A. Alshmimri, J. A. Reimer and O. M. Yaghi, Crystalline Dioxin-Linked Covalent Organic Frameworks from Irreversible Reactions, *J. Am. Chem. Soc.*, 2018, **140**, 12715–12719.

115 M. Lu, M. Zhang, C. G. Liu, J. Liu, L. J. Shang, M. Wang, J. N. Chang, S. L. Li and Y. Q. Lan, Stable Dioxin-Linked Metallophthalocyanine Covalent Organic Frameworks (COFs) as Photo-Coupled Electrocatalysts for CO_2 Reduction, *Angew. Chem., Int. Ed.*, 2021, **60**, 4864–4871.

116 Q. Zhi, W. Liu, R. Jiang, X. Zhan, Y. Jin, X. Chen, X. Yang, K. Wang, W. Cao, D. Qi and J. Jiang, Piperazine-Linked Metalphthalocyanine Frameworks for Highly Efficient Visible-Light-Driven H_2O_2 Photosynthesis, *J. Am. Chem. Soc.*, 2022, **144**, 21328–21336.

117 Y. Yue, H. Li, H. Chen and N. Huang, Piperazine-Linked Covalent Organic Frameworks with High Electrical Conductivity, *J. Am. Chem. Soc.*, 2022, **144**, 2873–2878.

118 M. Wang, M. Ballabio, M. Wang, H. H. Lin, B. P. Biswal, X. Han, S. Paasch, E. Brunner, P. Liu, M. Chen, M. Bonn, T. Heine, S. Zhou, E. Canovas, R. Dong and X. Feng, Unveiling Electronic Properties in Metal-Phthalocyanine-Based Pyrazine-Linked Conjugated Two-Dimensional Covalent Organic Frameworks, *J. Am. Chem. Soc.*, 2019, **141**, 16810–16816.

119 F. Haase, E. Troschke, G. Savasci, T. Banerjee, V. Duppel, S. Dorfler, M. M. J. Grundei, A. M. Burow, C. Ochsenfeld, S. Kaskel and B. V. Lotsch, Topochemical conversion of an imine- into a thiazole-linked covalent organic framework enabling real structure analysis, *Nat. Commun.*, 2018, **9**, 2600.

120 V. Singh, J. Kim, B. Kang, J. Moon, S. Kim, W. Y. Kim and H. R. Byon, Thiazole-Linked Covalent Organic Framework Promoting Fast Two-Electron Transfer for Lithium-Organic Batteries, *Adv. Energy Mater.*, 2021, **11**, 2003735.

121 R.-J. Wei, H.-G. Zhou, Z.-Y. Zhang, G.-H. Ning and D. Li, Copper (I)–Organic Frameworks for Catalysis: Networking Metal Clusters with Dynamic Covalent Chemistry, *CCS Chem.*, 2020, **2**, 2045–2053.

122 R.-J. Wei, M. Xie, R.-Q. Xia, J. Chen, H. -J Hu, G.-H. Ning and D. Li, Gold(I)-Organic Frameworks as Catalysts for Carboxylation of Alkynes with CO_2, *J. Am. Chem. Soc.*, 2023, **145**, 22720–22727.

123 P.-Y. You, K.-M. Mo, Y.-M. Wang, Q. Gao, X.-C. Lin, J.-T. Lin, M. Xie, G.-H. Ning and D. Li, Reversible modulation of interlayer stacking in 2D copper-organic frameworks for tailoring porosity and photocatalytic activity, *Nat. Commun.*, 2023, **15**, 194.

124 X.-C. Lin, Y.-M. Wang, X. Chen, P.-Y. You, K.-M. Mo, G.-H. Ning and D. Li, A photosensitizing metal–organic framework as a tandem reaction catalyst for primary alcohols from terminal alkenes and alkynes, *Angew. Chem., Int. Ed.*, 2023, **62**, e202306497.

125 H. Duan, X. Chen, Y.-N. Yang, J. Zhao, X.-C. Lin, W.-J. Tang, Q. Gao, G.-N. Ning and D. Li, Tailoring stability, catalytic activity and selectivity of covalent metal–organic frameworks *via* steric modification of metal nodes, *J. Mater. Chem. A*, 2023, **11**, 12777–12783.

126 H. G. Zhou, R.-Q. Xia, J. Zheng, D. Yuan, G.-N. Ning and D. Li, Acid-triggered interlayer sliding of two dimensional copper(I)–organic frameworks: more metal sites for catalysis, *Chem. Sci.*, 2021, **12**, 6280–6286.

127 X. Chen, J.-Y. Song, J. Zheng, Y.-M. Wang, J. Luo, P. Weng, B.-C. Cai, X.-C. Lin, G.-H. Ning and D. Li, Metal Variance in Multivariate Metal–Organic Frameworks for Boosting Catalytic Conversion of CO_2, *J. Am. Chem. Soc.*, 2024, **146**, 19271–19278.

128 J. Luo, X. Luo, M. Xie, J.-T. Lin, J. Pang, N. Yin, Y.-Y. Li, G.-H. Ning and D. Li, Molecular regulation of metal-

organic frameworks for rapid and efficient extraction of uranium from seawater, *Sci. China: Chem.*, 2025, **68**, 1906–1915.

129 Z. Wang and S. M. Cohen, Postsynthetic modification of metal-organic frameworks, *Chem. Soc. Rev.*, 2009, **38**, 1315–1329.

130 S. Mandal, S. Natarajan, P. Mani and A. Pankajakshan, Post-Synthetic Modification of Metal–Organic Frameworks Toward Applications, *Adv. Funct. Mater.*, 2020, **31**, 2006291.

131 J. L. Segura, S. Royuela and M. Mar Ramos, Post-synthetic modification of covalent organic frameworks, *Chem. Soc. Rev.*, 2019, **48**, 3903–3945.

132 N. A. Rejali, M. Dinari and Y. Wang, Post-synthetic modifications of covalent organic frameworks (COFs) for diverse applications, *Chem. Commun.*, 2023, **59**, 11631–11647.

133 L. Cusin, H. Peng, A. Ciesielski and P. Samori, Chemical Conversion and Locking of the Imine Linkage: Enhancing the Functionality of Covalent Organic Frameworks, *Angew. Chem., Int. Ed.*, 2021, **60**, 14236–14250.

134 S. Abednatanzi, P. Gohari Derakhshandeh, H. Depauw, F. X. Coudert, H. Vrielinck, P. Van Der Voort and K. Leus, Mixed-metal metal-organic frameworks, *Chem. Soc. Rev.*, 2019, **48**, 2535–2565.

135 L. Chen, H. F. Wang, C. Li and Q. Xu, Bimetallic metal-organic frameworks and their derivatives, *Chem. Sci.*, 2020, **11**, 5369–5403.

136 S. Das, H. Kim and K. Kim, Metathesis in single crystal: Complete and reversible exchange of metal ions constituting the frameworks of metal–organic frameworks, *J. Am. Chem. Soc.*, 2009, **131**, 3814–3815.

137 X. Song, S. Jeong, D. Kim and M. S. Lah, Transmetalations in two metal–organic frameworks with different framework flexibilities: Kinetics and core–shell heterostructure, *CrystEngComm*, 2012, **14**, 5753–5756.

138 C. K. Brozek and M. Dincă, Ti$^{(3+)}$-, V$^{(2+/3+)}$-, Cr$^{(2+/3+)}$-, Mn$^{(2+)}$-, and Fe$^{(2+)}$-substituted MOF-5 and redox reactivity in Cr- and Fe-MOF-5, *J. Am. Chem. Soc.*, 2013, **135**, 12886–12891.

139 T. Li, M. T. Kozlowski, E. A. Doud, M. N. Blakely and N. L. Rosi, Stepwise ligand exchange for the preparation of a family of mesoporous MOFs, *J. Am. Chem. Soc.*, 2013, **135**, 11688–11691.

140 H. Fei, J. F. Cahill, K. A. Prather and S. M. Cohen, Tandem postsynthetic metal ion and ligand exchange in zeolitic imidazolate frameworks, *Inorg. Chem.*, 2013, **52**, 4011–4016.

141 M. Kim, J. F. Cahill, Y. Su, K. A. Prather and S. M. Cohen, Postsynthetic ligand exchange as a route to functionalization of 'inert' metal–organic frameworks, *Chem. Sci.*, 2012, **3**, 126–130.

142 M. Kim, J. F. Cahill, H. Fei, K. A. Prather and S. M. Cohen, Postsynthetic ligand and cation exchange in robust metal-organic frameworks, *J. Am. Chem. Soc.*, 2012, **134**, 18082–18088.

143 C. Qian, Q. Y. Qi, G. F. Jiang, F. Z. Cui, Y. Tian and X. Zhao, Toward Covalent Organic Frameworks Bearing Three Different Kinds of Pores: The Strategy for Construction and COF-to-COF Transformation *via* Heterogeneous Linker Exchange, *J. Am. Chem. Soc.*, 2017, **139**, 6736–6743.

144 J. Xu, G. Feng, D. Ao, X. Li, M. Li, S. Lei and Y. Wang, Functional Covalent Organic Frameworks' Microspheres Synthesized by Self-Limited Dynamic Linker Exchange for Stationary Phases, *Adv. Mater.*, 2024, **36**, e2406256.

145 S. S. Y. Chui, S. M. F. Lo, J. P. H. Charmant, A. G. Orpen and I. D. Williams, A Chemically Functionalizable Nanoporous Material [$Cu_3(TMA)_2(H_2O)_3$]n, *Science*, 1999, **283**, 1148–1150.

146 E. D. Bloch, D. Britt, C. Lee, C. J. Doonan, F. J. Uribe-Romo, H. Furukawa, J. R. Long and O. M. Yaghi, Metal insertion in a microporous metal–organic framework lined with 2, 2'-bipyridine, *J. Am. Chem. Soc.*, 2010, **132**, 14382–14384.

147 K. Manna, T. Zhang and W. Lin, Postsynthetic metalation of bipyridyl-containing metal-organic frameworks for highly efficient catalytic organic transformations, *J. Am. Chem. Soc.*, 2014, **136**, 6566–6569.

148 Q. Sun, B. Aguila, J. Perman, N. Nguyen and S. Ma, Flexibility Matters: Cooperative Active Sites in Covalent Organic Framework and Threaded Ionic Polymer, *J. Am. Chem. Soc.*, 2016, **138**, 15790–15796.

149 W. Liu, Y. Zhang, J. Wang, X. Shang, C. Zhang and Q. Wang, Advances of functionalized bipyridine-based covalent-organic frameworks for boosting photocatalysis, *Coord. Chem. Rev.*, 2024, **516**, 215997.

150 A. Jati, K. Dey, M. Nurhuda, M. A. Addicoat, R. Banerjee and B. Maji, Dual Metalation in a Two-Dimensional Covalent Organic Framework for Photocatalytic C-N Cross-Coupling Reactions, *J. Am. Chem. Soc.*, 2022, **144**, 7822–7833.

151 W. Tu, Y. Xu, S. Yin and R. Xu, Rational Design of Catalytic Centers in Crystalline Frameworks, *Adv. Mater.*, 2018, **30**, 1707582.

152 L. H. Li, X. L. Feng, X. H. Cui, Y. X. Ma, S. Y. Ding and W. Wang, Salen-Based Covalent Organic Framework, *J. Am. Chem. Soc.*, 2017, **139**, 6042–6045.

153 A. M. Shultz, A. A. Sarjeant, O. K. Farha, J. T. Hupp and S. T. Nguyen, Post-synthesis modification of a metal-organic framework to form metallosalen-containing MOF materials, *J. Am. Chem. Soc.*, 2011, **133**, 13252–13255.

154 Z. Wang and S. M. Cohen, Postsynthetic Covalent Modification of a Neutral Metal–Organic Framework, *J. Am. Chem. Soc.*, 2007, **129**, 12368–12369.

155 A. Nagai, Z. Guo, X. Feng, S. Jin, X. Chen, X. Ding and D. Jiang, Pore surface engineering in covalent organic frameworks, *Nat. Commun.*, 2011, **2**, 536.

156 A. N. Hong, H. Yang, X. Bu and P. Feng, Pore space partition of metal-organic frameworks for gas storage and separation, *EnergyChem*, 2022, **4**, 100080.

157 Q. G. Zhai, X. Bu, X. Zhao, D. S. Li and P. Feng, Pore Space Partition in Metal-Organic Frameworks, *Acc. Chem. Res.*, 2017, **50**, 407–417.

158 Q. G. Zhai, X. Bu, C. Mao, X. Zhao, L. Daemen, Y. Cheng, A. J. Ramirez-Cuesta and P. Feng, An ultra-tunable platform for molecular engineering of high-performance crystalline porous materials, *Nat. Commun.*, 2016, **7**, 13645.

159 S. T. Zheng, X. Zhao, S. Lau, A. Fuhr, P. Feng and X. Bu, Entrapment of metal clusters in metal-organic framework channels by extended hooks anchored at open metal sites, *J. Am. Chem. Soc.*, 2013, **135**, 10270–10273.

160 X. Zhao, X. Bu, Q. G. Zhai, H. Tran and P. Feng, Pore space partition by symmetry-matching regulated ligand insertion and dramatic tuning on carbon dioxide uptake, *J. Am. Chem. Soc.*, 2015, **137**, 1396–1399.

161 X. Xu, X. Wu, K. Xu, H. Xu, H. Chen and N. Huang, Pore partition in two-dimensional covalent organic frameworks, *Nat. Commun.*, 2023, **14**, 3360.

162 M. Hao, Y. Xie, M. Lei, X. Liu, Z. Chen, H. Yang, G. I. N. Waterhouse, S. Ma and X. Wang, Pore Space Partition Synthetic Strategy in Imine-linked Multivariate Covalent Organic Frameworks, *J. Am. Chem. Soc.*, 2024, **146**, 1904–1913.

163 W. Zhang, H. Jiang, Y. Liu, Y. Hu, A. S. Palakkal, Y. Zhou, M. Sun, E. Du, W. Gong, Q. Zhang, J. Jiang, J. Dong, Y. Liu, Y. Zhu, Y. Cui and X. Duan, Metal-halide porous framework superlattices, *Nature*, 2025, **638**, 418–424.

164 R.-B. Lin, S. Xiang, W. Zhou and B. Chen, Microporous Metal-Organic Framework Materials for Gas Separation, *Chem*, 2020, **6**, 337–363.

165 S. J. Geier, J. A. Mason, E. D. Bloch, W. L. Queen, M. R. Hudson, C. M. Brown and J. R. Long, Selective adsorption of ethylene over ethane and propylene over propane in the metal–organic frameworks M_2(dobdc) (M = Mg, Mn, Fe, Co, Ni, Zn), *Chem. Sci.*, 2013, **4**, 2054–2061.

166 S. Qiu, M. Xue and G. Zhu, Metal-organic framework membranes: from synthesis to separation application, *Chem. Soc. Rev.*, 2014, **43**, 6116–6140.

167 A. U. Czaja, N. Trukhan and U. Muller, Industrial applications of metal-organic frameworks, *Chem. Soc. Rev.*, 2009, **38**, 1284–1293.

168 K. Adil, Y. Belmabkhout, R. S. Pillai, A. Cadiau, P. M. Bhatt, A. H. Assen, G. Maurin and M. Eddaoudi, Gas/vapour separation using ultra-microporous metal-organic frameworks: insights into the structure/separation relationship, *Chem. Soc. Rev.*, 2017, **46**, 3402–3430.

169 S. Ma and H. C. Zhou, Gas storage in porous metal-organic frameworks for clean energy applications, *Chem. Commun.*, 2010, **46**, 44–53.

170 L. J. Murray, M. Dinca and J. R. Long, Hydrogen storage in metal-organic frameworks, *Chem. Soc. Rev.*, 2009, **38**, 1294–1314.

171 M. P. Suh, H. J. Park, T. K. Prasad and D. W. Lim, Hydrogen storage in metal-organic frameworks, *Chem. Rev.*, 2012, **112**, 782–835.

172 J. A. Mason, M. Veenstra and J. R. Long, Evaluating metal–organic frameworks for natural gas storage, *Chem. Sci.*, 2014, **5**, 32–51.

173 B. Li, H.-M. Wen, W. Zhou, J. Q. Xu and B. Chen, Porous Metal-Organic Frameworks: Promising Materials for Methane Storage, *Chem*, 2016, **1**, 557–580.

174 Y. He, W. Zhou, G. Qian and B. Chen, Methane storage in metal-organic frameworks, *Chem. Soc. Rev.*, 2014, **43**, 5657–5678.

175 A. R. Millward and O. M. Yaghi, Metal–Organic Frameworks with Exceptionally High Capacity for Storage of Carbon Dioxide at Room Temperature, *J. Am. Chem. Soc.*, 2005, **127**, 17998–17999.

176 K. Sumida, D. L. Rogow, J. A. Mason, T. M. McDonald, E. D. Bloch, Z. R. Herm, T. H. Bae and J. R. Long, Carbon dioxide capture in metal-organic frameworks, *Chem. Rev.*, 2012, **112**, 724–781.

177 N. L. Rosi, J. Eckert, M. Eddaoudi, D. T. Vodak, J. Kim, M. O'Keeffe and O. M. Yaghi, Hydrogen Storage in Microporous Metal-Organic Frameworks, *Science*, 2003, **300**, 1127–1129.

178 D. Yuan, D. Zhao, D. Sun and H. C. Zhou, An isoreticular series of metal-organic frameworks with dendritic hexacarboxylate ligands and exceptionally high gas-uptake capacity, *Angew. Chem., Int. Ed.*, 2010, **49**, 5357–5361.

179 Y. Yan, X. Lin, S. Yang, A. J. Blake, A. Dailly, N. R. Champness, P. Hubberstey and M. Schroder, Exceptionally high H_2 storage by a metal-organic polyhedral framework, *Chem. Commun.*, 2009, 1025–1027.

180 O. K. Farha, C. E. Wilmer, I. Eryazici, B. G. Hauser, P. A. Parilla, K. O'Neill, A. A. Sarjeant, S. T. Nguyen, R. Q. Snurr and J. T. Hupp, Designing higher surface area metal-organic frameworks: are triple bonds better than phenyls?, *J. Am. Chem. Soc.*, 2012, **134**, 9860–9863.

181 O. K. Farha, A. O. Yazaydin, I. Eryazici, C. D. Malliakas, B. G. Hauser, M. G. Kanatzidis, S. T. Nguyen, R. Q. Snurr and J. T. Hupp, De novo synthesis of a metal-organic framework material featuring ultrahigh surface area and gas storage capacities, *Nat. Chem.*, 2010, **2**, 944–948.

182 S. S. Han, H. Furukawa, O. M. Yaghi and W. A. Goddard, Covalent organic frameworks as exceptional hydrogen storage materials, *J. Am. Chem. Soc.*, 2008, **130**, 11580–11581.

183 R. Zacharia, D. Cossement, L. Lafi and R. Chahine, Volumetric hydrogen sorption capacity of monoliths prepared by mechanical densification of MOF-177, *J. Mater. Chem.*, 2010, **20**, 2145–2451.

184 S. S. Kaye, A. Dailly, O. M. Yaghi and J. R. Long, Impact of Preparation and Handling on the Hydrogen Storage Properties of Zn_4O(1,4-benzenedicarboxylate)$_3$ (MOF-5), *J. Am. Chem. Soc.*, 2007, **129**, 14176–14177.

185 Y. Pramudya and J. L. Mendoza-Cortes, Design Principles for High H_2 Storage Using Chelation of Abundant Transition Metals in Covalent Organic Frameworks for 0-700 bar at 298 K, *J. Am. Chem. Soc.*, 2016, **138**, 15204–15213.

186 S. Yang, G. S. Martin, J. J. Titman, A. J. Blake, D. R. Allan, N. R. Champness and M. Schroder, Pore with gate: enhancement of the isosteric heat of adsorption of dihydrogen *via* postsynthetic cation exchange in metal-organic frameworks, *Inorg. Chem.*, 2011, **50**, 9374–9384.

187 Y. Peng, V. Krungleviciute, I. Eryazici, J. T. Hupp, O. K. Farha and T. Yildirim, Methane storage in metal-organic frameworks: current records, surprise findings, and challenges, *J. Am. Chem. Soc.*, 2013, **135**, 11887–11894.

188 B. Li, H. M. Wen, H. Wang, H. Wu, M. Tyagi, T. Yildirim, W. Zhou and B. Chen, A porous metal-organic framework with dynamic pyrimidine groups exhibiting record high methane storage working capacity, *J. Am. Chem. Soc.*, 2014, **136**, 6207–6210.

189 Y. Yin, Y. Zhang, X. Zhou, B. Gui, W. Q. Wang, W. T. Jiang, Y. B. Zhang, J. L. Sun and C. Wang, Ultrahigh–surface area covalent organic frameworks for methane adsorption, *Science*, 2024, **386**, 693–696.

190 H. Li, L. Li, R. B. Lin, W. Zhou, Z. Zhang, S. Xiang and B. Chen, Porous metal-organic frameworks for gas storage and separation: Status and challenges, *EnergyChem*, 2019, **1**, 100006.

191 A. Ebadi Amooghin, H. Sanaeepur, R. Luque, H. Garcia and B. Chen, Fluorinated metal-organic frameworks for gas separation, *Chem. Soc. Rev.*, 2022, **51**, 7427–7508.

192 L. Yang, S. Qian, X. Wang, X. Cui, B. Chen and H. Xing, Energy-efficient separation alternatives: metal-organic frameworks and membranes for hydrocarbon separation, *Chem. Soc. Rev.*, 2020, **49**, 5359–5406.

193 Y. Yang, L. Li, R. B. Lin, Y. Ye, Z. Yao, L. Yang, F. Xiang, S. Chen, Z. Zhang, S. Xiang and B. Chen, Ethylene/ethane separation in a stable hydrogen-bonded organic framework through a gating mechanism, *Nat. Chem.*, 2021, **13**, 933–939.

194 L. Li, R.-B. Lin, R. Krishna, H. Li, S. Xiang, H. Wu, J. Li, W. Zhou and B. Chen, Ethane/ethylene separation in a metal-organic framework with iron-peroxo sites, *Science*, 2018, **362**, 443–446.

195 R. B. Lin, L. Li, H. L. Zhou, H. Wu, C. He, S. Li, R. Krishna, J. Li, W. Zhou and B. Chen, Molecular sieving of ethylene from ethane using a rigid metal-organic framework, *Nat. Mater.*, 2018, **17**, 1128–1133.

196 B. Chen, C. Liang, J. Yang, D. S. Contreras, Y. L. Clancy, E. B. Lobkovsky, O. M. Yaghi and S. Dai, A microporous metal-organic framework for gas-chromatographic separation of alkanes, *Angew. Chem., Int. Ed.*, 2006, **45**, 1390–1393.

197 P. S. Barcia, F. Zapata, J. A. C. Silva, A. E. Rodrigues and B. Chen, Kinetic Separation of Hexane Isomers by Fixed-Bed Adsorption with a Microporous Metal–Organic Framework, *J. Phys. Chem. B*, 2007, **111**, 6101–6103.

198 X. Cui, K. Chen, H. Xing, Q. Yang, R. Krishna, Z. Bao, H. Wu, W. Zhou, X. Dong, Y. Han, B. Li, Q. Ren, M. J. Zaworotko and B. Chen, Pore chemistry and size control in hybrid porous materials for acetylene capture from ethylene, *Science*, 2016, **353**, 141–144.

199 F. Luo, C. Yan, L. Dang, R. Krishna, W. Zhou, H. Wu, X. Dong, Y. Han, T. L. Hu, M. O'Keeffe, L. Wang, M. Luo, R. B. Lin and B. Chen, UTSA-74: A MOF-74 Isomer with Two Accessible Binding Sites per Metal Center for Highly Selective Gas Separation, *J. Am. Chem. Soc.*, 2016, **138**, 5678–5684.

200 Z. Niu, X. Cui, T. Pham, G. Verma, P. C. Lan, C. Shan, H. Xing, K. A. Forrest, S. Suepaul, B. Space, A. Nafady, A. M. Al-Enizi and S. Ma, A MOF-based Ultra-Strong Acetylene Nano-trap for Highly Efficient C_2H_2/CO_2 Separation, *Angew. Chem., Int. Ed.*, 2021, **60**, 5283–5288.

201 Y. Ye, S. Xian, H. Cui, K. Tan, L. Gong, B. Liang, T. Pham, H. Pandey, R. Krishna, P. C. Lan, K. A. Forrest, B. Space, T. Thonhauser, J. Li and S. Ma, Metal-Organic Framework Based Hydrogen-Bonding Nanotrap for Efficient Acetylene Storage and Separation, *J. Am. Chem. Soc.*, 2022, **144**, 1681–1689.

202 C. X. Chen, Z. W. Wei, T. Pham, P. C. Lan, L. Zhang, K. A. Forrest, S. Chen, A. M. Al-Enizi, A. Nafady, C. Y. Su and S. Ma, Nanospace Engineering of Metal-Organic Frameworks through Dynamic Spacer Installation of Multifunctionalities for Efficient Separation of Ethane from Ethane/Ethylene Mixtures, *Angew. Chem., Int. Ed.*, 2021, **60**, 9680–9685.

203 Y. Ye, Y. Xie, Y. Shi, L. Gong, J. Phipps, A. M. Al-Enizi, A. Nafady, B. Chen and S. Ma, A Microporous Metal-Organic Framework with Unique Aromatic Pore Surfaces for High Performance C_2H_6/C_2H_4 Separation, *Angew. Chem., Int. Ed.*, 2023, **62**, e202302564.

204 H. Fan, H. Wang, M. Peng, H. Meng, A. Mundstock, A. Knebel and J. Caro, Pore-in-Pore Engineering in a Covalent Organic Framework Membrane for Gas Separation, *ACS Nano*, 2023, **17**, 7584–7594.

205 B. Aguila, Q. Sun, X. Wang, E. O'Rourke, A. M. Al-Enizi, A. Nafady and S. Ma, Lower Activation Energy for Catalytic Reactions through Host-Guest Cooperation within Metal-Organic Frameworks, *Angew. Chem., Int. Ed.*, 2018, **57**, 10107–10111.

206 G. Férey, C. Mellot-Draznieks, C. Serre, F. Millange, J. Dutour, S. Surblé and I. Margiolaki, A Chromium Terephthalate-Based Solid with Unusually Large Pore Volumes and Surface Area, *Science*, 2005, **309**, 2040–2042.

207 Y. Fu, L. Xu, H. Shen, H. Yang, F. Zhang, W. Zhu and M. Fan, Tunable catalytic properties of multi-metal–organic frameworks for aerobic styrene oxidation, *Chem. Eng. J.*, 2016, **299**, 135–141.

208 S. Zhao, Y. Wang, J. Dong, C.-T. He, H. Yin, P. An, K. Zhao, X. Zhang, C. Gao, L. Zhang, J. Lv, J. Wang, J. Zhang, A. M. Khattak, N. A. Khan, Z. Wei, J. Zhang, S. Liu, H. Zhao and Z. Tang, Ultrathin metal–organic framework nanosheets for electrocatalytic oxygen evolution, *Nat. Energy*, 2016, **1**, 16184.

209 Y. Lee, S. Kim, J. K. Kang and S. M. Cohen, Photocatalytic CO_2 reduction by a mixed metal (Zr/Ti), mixed ligand metal-organic framework under visible light irradiation, *Chem. Commun.*, 2015, **51**, 5735–5738.

210 C. Zhang, C. Xie, Y. Gao, X. Tao, C. Ding, F. Fan and H. L. Jiang, Charge Separation by Creating Band Bending in Metal-Organic Frameworks for Improved Photocatalytic Hydrogen Evolution, *Angew. Chem., Int. Ed.*, 2022, **61**, e202204108.

211 K. Sun, Y. Huang, F. Sun, Q. Wang, Y. Zhou, J. Wang, Q. Zhang, X. Zheng, F. Fan, Y. Luo, J. Jiang and H. L. Jiang, Dynamic structural twist in metal-organic frameworks enhances solar overall water splitting, *Nat. Chem.*, 2024, **16**, 1638–1646.

212 G. Yang, D. Wang, Y. Wang, W. Hu, S. Hu, J. Jiang, J. Huang and H. L. Jiang, Modulating the Primary and Secondary Coordination Spheres of Single Ni(II) Sites in Metal-Organic Frameworks for Boosting Photocatalysis, *J. Am. Chem. Soc.*, 2024, **146**, 10798–10805.

213 K. Sun, Y. Huang, Q. Wang, W. Zhao, X. Zheng, J. Jiang and H. L. Jiang, Manipulating the Spin State of Co Sites in Metal-Organic Frameworks for Boosting CO_2 Photoreduction, *J. Am. Chem. Soc.*, 2024, **146**, 3241–3249.

214 H. Wang, X. Liu, W. Yang, G. Mao, Z. Meng, Z. Wu and H. L. Jiang, Surface-Clean Au_{25} Nanoclusters in Modulated Microenvironment Enabled by Metal-Organic Frameworks for Enhanced Catalysis, *J. Am. Chem. Soc.*, 2022, **144**, 22008–22017.

215 H. Wang, X. Zhang, W. Zhang, M. Zhou and H. L. Jiang, Heteroatom-Doped Ag_{25} Nanoclusters Encapsulated in Metal-Organic Frameworks for Photocatalytic Hydrogen Production, *Angew. Chem., Int. Ed.*, 2024, **63**, e202401443.

216 L. Wen, K. Sun, X. Liu, W. Yang, L. Li and H. L. Jiang, Electronic State and Microenvironment Modulation of Metal Nanoparticles Stabilized by MOFs for Boosting Electrocatalytic Nitrogen Reduction, *Adv. Mater.*, 2023, **35**, e2210669.

217 S. Wang, Z. Ai, X. Niu, W. Yang, R. Kang, Z. Lin, A. Waseem, L. Jiao and H. L. Jiang, Linker Engineering of Sandwich-Structured Metal-Organic Framework Composites for Optimized Photocatalytic H_2 Production, *Adv. Mater.*, 2023, **35**, e2302512.

218 Z. Niu, W. D. C. Bhagya Gunatilleke, Q. Sun, P. C. Lan, J. Perman, J.-G. Ma, Y. Cheng, B. Aguila and S. Ma, Metal-Organic Framework Anchored with a Lewis Pair as a New Paradigm for Catalysis, *Chem*, 2018, **4**, 2587–2599.

219 Z. Niu, W. Zhang, P. C. Lan, B. Aguila and S. Ma, Promoting Frustrated Lewis Pairs for Heterogeneous Chemoselective Hydrogenation *via* the Tailored Pore Environment within Metal-Organic Frameworks, *Angew. Chem., Int. Ed.*, 2019, **58**, 7420–7424.

220 Z. M. Xu, Z. Hu, Y. Huang, S. J. Bao, Z. Niu, J. P. Lang, A. M. Al-Enizi, A. Nafady and S. Ma, Introducing Frustrated Lewis Pairs to Metal-Organic Framework for Selective Hydrogenation of N-Heterocycles, *J. Am. Chem. Soc.*, 2023, **145**, 14994–15000.

221 Y. Zhang, S. Chen, A. M. Al-Enizi, A. Nafady, Z. Tang and S. Ma, Chiral Frustrated Lewis Pair@Metal-Organic Framework as a New Platform for Heterogeneous Asymmetric Hydrogenation, *Angew. Chem., Int. Ed.*, 2023, **62**, e202213399.

222 Y. Zhang, Y. Jiang, A. Nafady, Z. Tang, A. M. Al-Enizi, K. Tan and S. Ma, Incorporation of Chiral Frustrated Lewis Pair into Metal-Organic Framework with Tailored Microenvironment for Heterogeneous Enantio- and Chemoselective Hydrogenation, *ACS Cent. Sci.*, 2023, **9**, 1692–1701.

223 Y. Zhang, J. Guo, P. VanNatta, Y. Jiang, J. Phipps, R. Roknuzzaman, H. Rabaa, K. Tan, T. AlShahrani and S. Ma, Metal-Free Heterogeneous Asymmetric Hydrogenation of Olefins Promoted by Chiral Frustrated Lewis Pair Framework, *J. Am. Chem. Soc.*, 2024, **146**, 979–987.

224 Q. Sun, Y. Tang, B. Aguila, S. Wang, F. S. Xiao, P. K. Thallapally, A. M. Al-Enizi, A. Nafady and S. Ma, Reaction Environment Modification in Covalent Organic Frameworks for Catalytic Performance Enhancement, *Angew. Chem., Int. Ed.*, 2019, **58**, 8670–8675.

225 Q. Sun, C. W. Fu, B. Aguila, J. Perman, S. Wang, H. Y. Huang, F. S. Xiao and S. Ma, Pore Environment Control and Enhanced Performance of Enzymes Infiltrated in Covalent Organic Frameworks, *J. Am. Chem. Soc.*, 2018, **140**, 984–992.

226 Q. Sun, B. Aguila, P. C. Lan and S. Ma, Tuning Pore Heterogeneity in Covalent Organic Frameworks for Enhanced Enzyme Accessibility and Resistance against Denaturants, *Adv. Mater.*, 2019, **31**, e1900008.

227 I. Simonsson, P. Gardhagen, M. Andren, P. L. Tam and Z. Abbas, Experimental investigations into the irregular synthesis of iron(iii) terephthalate metal-organic frameworks MOF-235 and MIL-101, *Dalton Trans.*, 2021, **50**, 4976–4985.

228 E. Haque, J. W. Jun and S. H. Jhung, Adsorptive removal of methyl orange and methylene blue from aqueous solution with a metal-organic framework material, iron terephthalate (MOF-235), *J. Hazard. Mater.*, 2011, **185**, 507–511.

229 S. C. Moore and M. L. Sarazen, Stability and kinetics of iron-terephthalate MOFs with diverse structures in aqueous pollutant degradation, *AIChE J.*, 2023, **69**, e18205.

230 Y. Peng, H. Huang, Y. Zhang, C. Kang, S. Chen, L. Song, D. Liu and C. Zhong, A versatile MOF-based trap for heavy metal ion capture and dispersion, *Nat. Commun.*, 2018, **9**, 187.

231 H. Furukawa, F. Gandara, Y. B. Zhang, J. Jiang, W. L. Queen, M. R. Hudson and O. M. Yaghi, Water adsorption in porous metal-organic frameworks and related materials, *J. Am. Chem. Soc.*, 2014, **136**, 4369–4381.

232 J. Jiang, F. Gandara, Y. B. Zhang, K. Na, O. M. Yaghi and W. G. Klemperer, Superacidity in sulfated metal-organic framework-808, *J. Am. Chem. Soc.*, 2014, **136**, 12844–12847.

233 Q. Sun, B. Aguila, J. Perman, L. D. Earl, C. W. Abney, Y. Cheng, H. Wei, N. Nguyen, L. Wojtas and S. Ma, Postsynthetically Modified Covalent Organic Frameworks for Efficient and Effective Mercury Removal, *J. Am. Chem. Soc.*, 2017, **139**, 2786–2793.

234 Q. Sun, B. Aguila, J. A. Perman, T. Butts, F.-S. Xiao and S. Ma, Integrating Superwettability within Covalent Organic Frameworks for Functional Coating, *Chem*, 2018, **4**, 1726–1739.

235 M. Carboni, C. W. Abney, S. Liu and W. Lin, Highly porous and stable metal–organic frameworks for uranium extraction, *Chem. Sci.*, 2013, **4**, 2396–2402.

236 C. H. Hendon, A. J. Rieth, M. D. Korzynski and M. Dinca, Grand Challenges and Future Opportunities for Metal-Organic Frameworks, *ACS Cent. Sci.*, 2017, **3**, 554–563.

237 H. Yang, M. Hao, Y. Xie, X. Liu, Y. Liu, Z. Chen, X. Wang, G. I. N. Waterhouse and S. Ma, Tuning Local Charge

Distribution in Multicomponent Covalent Organic Frameworks for Dramatically Enhanced Photocatalytic Uranium Extraction, *Angew. Chem., Int. Ed.*, 2023, **62**, e202303129.

238 Y. Xie, Q. Rong, F. Mao, S. Wang, Y. Wu, X. Liu, M. Hao, Z. Chen, H. Yang, G. I. N. Waterhouse, S. Ma and X. Wang, Engineering the pore environment of antiparallel stacked covalent organic frameworks for capture of iodine pollutants, *Nat. Commun.*, 2024, **15**, 2671.

239 M. Hao, Z. Chen, H. Yang, G. I. N. Waterhouse, S. Ma and X. Wang, Pyridinium salt-based covalent organic framework with well-defined nanochannels for efficient and selective capture of aqueous $^{99}TcO_4^-$, *Sci. Bull.*, 2022, **67**, 924–932.

240 Q. Sun, L. Zhu, B. Aguila, P. K. Thallapally, C. Xu, J. Chen, S. Wang, D. Rogers and S. Ma, Optimizing radionuclide sequestration in anion nanotraps with record pertechnetate sorption, *Nat. Commun.*, 2019, **10**, 1646.

241 Q. Sun, B. Aguila, L. D. Earl, C. W. Abney, L. Wojtas, P. K. Thallapally and S. Ma, Covalent Organic Frameworks as a Decorating Platform for Utilization and Affinity Enhancement of Chelating Sites for Radionuclide Sequestration, *Adv. Mater.*, 2018, **30**, e1705479.

242 X. Yan, Y. Zhao, G. Cao, X. Li, C. Gao, L. Liu, S. Ahmed, F. Altaf, H. Tan, X. Ma, Z. Xie and H. Zhang, 2D Organic Materials: Status and Challenges, *Adv. Sci.*, 2023, **10**, e2203889.

243 J. Guo and D. Jiang, Covalent Organic Frameworks for Heterogeneous Catalysis: Principle, Current Status, and Challenges, *ACS Cent. Sci.*, 2020, **6**, 869–879.

244 P. Kumar, B. Anand, Y. F. Tsang, K. H. Kim, S. Khullar and B. Wang, Regeneration, degradation, and toxicity effect of MOFs: Opportunities and challenges, *Environ. Res.*, 2019, **176**, 108488.

245 X. Kang, E. R. Stephens, B. M. Spector-Watts, Z. Li, Y. Liu, L. Liu and Y. Cui, Challenges and opportunities for chiral covalent organic frameworks, *Chem. Sci.*, 2022, **13**, 9811–9832.

246 Q. Qian, P. A. Asinger, M. J. Lee, G. Han, K. Mizrahi Rodriguez, S. Lin, F. M. Benedetti, A. X. Wu, W. S. Chi and Z. P. Smith, MOF-Based Membranes for Gas Separations, *Chem. Rev.*, 2020, **120**, 8161–8266.

247 C. Zhang, B. H. Wu, M. Q. Ma, Z. Wang and Z. K. Xu, Ultrathin metal/covalent-organic framework membranes towards ultimate separation, *Chem. Soc. Rev.*, 2019, **48**, 3811–3841.

248 L. Huang, J. Yang, Y. Zhao, H. Miyata, M. Han, Q. Shuai and Y. Yamauchi, Monolithic Covalent Organic Frameworks with Hierarchical Architecture: Attractive Platform for Contaminant Remediation, *Chem. Mater.*, 2023, **35**, 2661–2682.

249 P. Albacete, M. Asgari, Y. Yang, A. N. Al-Shanks and D. Fairen-Jimenez, Self-Shaping Monolithic Reticular Materials: Ingredients for Success, *Adv. Funct. Mater.*, 2023, **34**, 2305979.

250 X. Qi, K. Liu and Z. Chang, Beyond powders: Monoliths on the basis of metal-organic frameworks (MOFs), *Chem. Eng. J.*, 2022, **441**, 135953.

251 J. Yu, C. Mu, B. Yan, X. Qin, C. Shen, H. Xue and H. Pang, Nanoparticle/MOF composites: preparations and applications, *Mater. Horiz.*, 2017, **4**, 557–569.

252 M. Kalaj, K. C. Bentz, S. Ayala Jr, J. M. Palomba, K. S. Barcus, Y. Katayama and S. M. Cohen, MOF-Polymer Hybrid Materials: From Simple Composites to Tailored Architectures, *Chem. Rev.*, 2020, **120**, 8267–8302.

253 Y. Liu, W. Zhou, W. L. Teo, K. Wang, L. Zhang, Y. Zeng and Y. Zhao, Covalent-Organic-Framework-Based Composite Materials, *Chem*, 2020, **6**, 3172–3202.

254 B. Sun, Z. Sun, Y. Yang, X. L. Huang, S. C. Jun, C. Zhao, J. Xue, S. Liu, H. K. Liu and S. X. Dou, Covalent Organic Frameworks: Their Composites and Derivatives for Rechargeable Metal-Ion Batteries, *ACS Nano*, 2024, **18**, 28–66.

255 K. Neikha and A. Puzari, Metal-Organic Frameworks through the Lens of Artificial Intelligence: A Comprehensive Review, *Langmuir*, 2024, **40**, 21957–21975.

256 Z. Zheng, O. Zhang, H. L. Nguyen, N. Rampal, A. H. Alawadhi, Z. Rong, T. Head-Gordon, C. Borgs, J. T. Chayes and O. M. Yaghi, ChatGPT Research Group for Optimizing the Crystallinity of MOFs and COFs, *ACS Cent. Sci.*, 2023, **9**, 2161–2170.

257 Z. Zheng, O. Zhang, C. Borgs, J. T. Chayes and O. M. Yaghi, ChatGPT Chemistry Assistant for Text Mining and the Prediction of MOF Synthesis, *J. Am. Chem. Soc.*, 2023, **145**, 18048–18062.

258 Y. Kang, W. Lee, T. Bae, S. Han, H. Jang and J. Kim, Harnessing Large Language Models to Collect and Analyze Metal-Organic Framework Property Data Set, *J. Am. Chem. Soc.*, 2025, **147**, 3943–3958.

259 L. Gagliardi and O. M. Yaghi, Three Future Directions for Metal–Organic Frameworks, *Chem. Mater.*, 2023, **35**, 5711–5712.

260 Z. Zheng, N. Rampal, T. J. Inizan, C. Borgs, J. T. Chayes and O. M. Yaghi, Large language models for reticular chemistry, *Nat. Rev. Mater.*, 2025, **10**, 369–381.

261 Z. Zheng, A. H. Alawadhi, S. Chheda, S. E. Neumann, N. Rampal, S. Liu, H. L. Nguyen, Y. H. Lin, Z. Rong, J. I. Siepmann, L. Gagliardi, A. Anandkumar, C. Borgs, J. T. Chayes and O. M. Yaghi, Shaping the Water-Harvesting Behavior of Metal-Organic Frameworks Aided by Fine-Tuned GPT Models, *J. Am. Chem. Soc.*, 2023, **145**, 28284–28295.

262 Q. Ouyang, Y. Rong, G. Xia, Q. Chen, Y. Ma and Z. Liu, Integrating Humidity-Resistant and Colorimetric COF-on-MOF Sensors with Artificial Intelligence Assisted Data Analysis for Visualization of Volatile Organic Compounds Sensing, *Adv. Sci.*, 2025, **12**, 2411621.